Bulletin of the Seismological Society of America, Vol. 78, No. 1, pp. 188–217, February 1988

THE NORTHEASTERN OHIO EARTHQUAKE OF 31 JANUARY 1986: WAS IT INDUCED?

BY C. NICHOLSON, E. ROELOFFS, AND R. L. WESSON

ABSTRACT

On 31 January 1986, at 11:46 EST, an earthquake of m_b = 5.0 occurred about 40 km east of Cleveland, Ohio, and about 17 km south of the Perry Nuclear Power Plant. The earthquake was felt over a broad area, including 11 states, the District of Columbia, and parts of Ontario, Canada, caused intensity VI–VII at distances of 15 km, and generated relatively high accelerations (0.18 g) of short duration at the Perry plant. Thirteen aftershocks were detected as of 15 April, with six occurring within the first 8 days. Two of the aftershocks were felt. Magnitudes for the aftershocks ranged from about 0.5 to 2.5. Focal depths for all of the earthquakes ranged from 2 to 6 km. Except for one small earthquake, all of the aftershocks occurred in a very tight cluster with a north-northeast orientation. Focal mechanisms of the aftershocks exhibit predominantly oblique right-slip motion on nearly vertical nodal planes oriented N15° to 45°E, with a nearly horizontal *P* axis north of east.

Three deep waste disposal wells are currently operating within 15 km of the epicentral region and have been responsible for the injection of nearly 1.2 billion liters of fluid at pressures reaching 112 bars above ambient at a nominal depth of 1.8 km. Estimates of stress inferred from commercial hydrofracturing measurements suggest that the state of stress in northeastern Ohio is close to the theoretical threshold for failure along favorably oriented, preexisting fractures. This implies that effective stress conditions near the bottom of the two most active wells may be at or near the critical level for incipient failure. Two and, possibly, three earthquakes have occurred within less than 5 km from the wells since 1983. The relative distance to the main shock epicenter and its aftershocks (about 12 km), the lack of large numbers of small earthquakes typical of many induced sequences, the history of small to moderate earthquakes in the region prior to the initiation of injection, and the attenuation of the pressure field with distance from the injection wells, however, all argue for a "natural" origin for the 1986 earthquakes. In contrast, the proximity to failure conditions at the bottom of the well and the probable spatial association of at least one earthquake suggest that triggering by well activities cannot be precluded.

INTRODUCTION

Earthquake occurrence in the Eastern United States is still a far from fully explained phenomenon. Although stresses within plate interiors are now known to be as large, if not larger, than those found at plate margins (e.g., Sbar and Sykes, 1973; Zoback and Zoback, 1980), and measured strain rates are sufficient to produce large damaging earthquakes over long periods of time (Musman and Schmidt, 1986), it is still unclear as to why certain earthquakes occur when and where they do. A major handicap is the long repeat times between moderate to large earthquakes in the east, and the fact that only a few have occurred since extensive monitoring capabilities have become operational. With so little information available, every earthquake in the east becomes a valuable opportunity for further insight into the nature of intraplate seismicity. The magnitude m_b = 5.0 earthquake in northeastern Ohio on 31 January 1986 is a case in point. Because of its comparatively large size, the potential for aftershock activity, and because of its proximity to a major critical

facility, the Perry Nuclear Power Plant, a substantial response by the seismological community was initiated. Analog portable seismographs were operating within 10 hr of the main shock, and broadband, wide-dynamic range, digital instruments were recording data within 27 hr. The net result was that 49 stations were deployed by seven agencies or institutions.

Several issues were raised by the occurrence of the earthquake. Of major concern was whether the main shock indicated a level of seismic hazard in excess of that previously believed to exist in the region. The 31 January earthquake was the largest to occur in northeastern Ohio since records of earthquake activity began; however, approximately 30 earthquakes of smaller magnitude had previously been recorded in the area (Figure 1). The largest of these prior earthquakes was a comparable magnitude (m_b = 4.5 to 4.7) and occurred in 1943. Neither the 1943 earthquake nor the recent one in 1986 exhibited any manifestation of surface faulting, leaving open the question as to the structure(s) at depth responsible for the earthquakes.

Another aspect of concern was that the 31 January earthquake and its aftershock sequence may have been induced by adjacent high-pressure fluid injection of hazardous and nonhazardous waste. Three wells that penetrate into basement are currently operating within 15 km of the earthquake epicenters. The observation that a large volume of fluid has been pumped into these wells over the last 11 yr and the knowledge that under certain conditions such operations in other locations have triggered small to moderate size earthquakes led to the speculation that the injection wells may have played a significant role in triggering the recent earthquake activity.

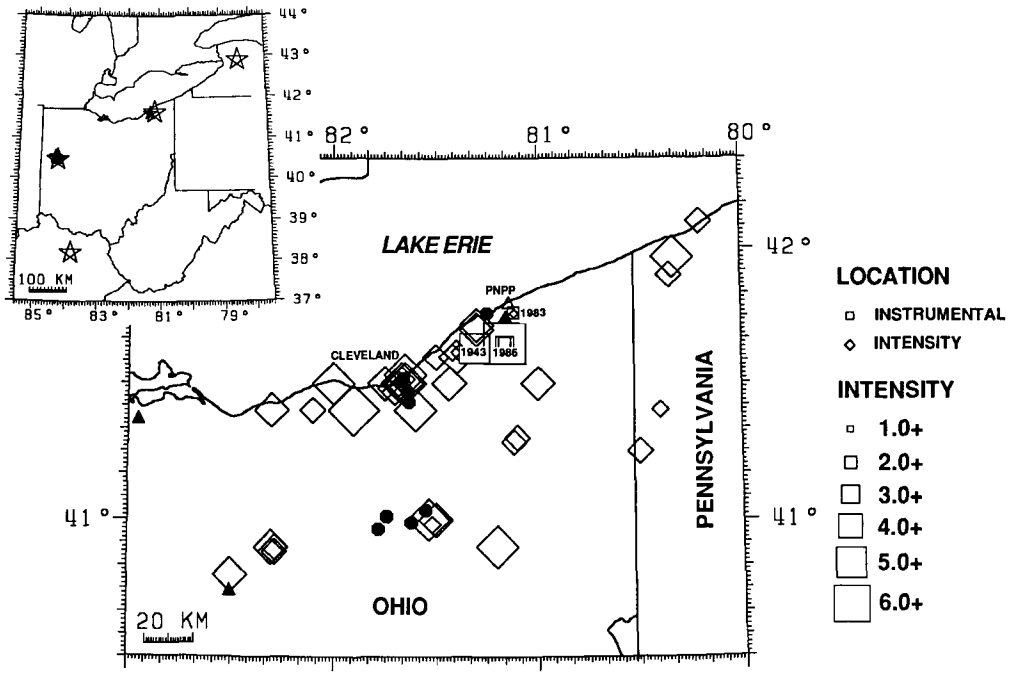

FIG. 1. Map of northeastern Ohio showing the location of the Perry Nuclear Power Plant (PNPP), the 31 January 1986 earthquake (large square), and significant historical seismicity (open symbols scaled according to intensity). Solid circles identify sites of solution salt mining, typically in operation from 1900 to 1940; solid triangles are deep waste injection wells drilled between 1968 and 1971. Most of the seismicity precedes initiation of injection activities. Diamonds are poorly located earthquakes, typically based on felt reports; squares are instrumentally located earthquakes. Modified from Stover *et al.* (1979). Recent regional earthquakes ($M \geqq 4.5$) are shown in the *inset*.

This paper consists of two parts resulting from various lines of investigation carried out by the U.S. Geological Survey and incorporates compilations of data from a number of different sources. The first is a basic study of the main shock and its aftershocks and includes locations, focal mechanisms, and information on previous historical seismicity. The second involves an investigation of the deep fluid injection wells and an assessment of the degree to which the wells may have influenced the local pattern of earthquake activity.

Earthquake Activity in Northeastern Ohio

Historical seismicity

Compilations of historical earthquakes in northeastern Ohio based on felt reports extend back to at least the mid-1820's. Instrumental recordings of local and regional earthquakes began in northeastern Ohio when John Carroll University, located in the outskirts of eastern Cleveland, started operation of its observatory in 1904. A seismicity map for this section of Ohio (Figure 1, Stover *et al.*, 1979) indicates a sustained level of activity, most of which occurred prior to the initiation of major injection operations in the late 1960's and early 1970's. Since 1823, the repeat time for felt earthquakes is about 5 to 6 yr, although earthquakes large enough to cause damage (intensity VI) are relatively rare. The magnitude 4.5 to 4.7 earthquake that occurred on 9 March 1943 was recently relocated using a regional velocity model appropriate for the Central United States (Dewey and Gordon, 1984). Its revised location (Figure 1, 41.628°N ± 14 km, 81.309°W ± 10 km) is only about 13 km west of the 1986 event. Thus, neither the size nor the location of the 1986 earthquake could be considered unusual.

Other earthquakes of even larger magnitude have occurred regionally within and around the state of Ohio (Figure 1, inset). The largest earthquake within the state was part of a swarm near Anna in 1937 and had a magnitude between 5.0 and 5.5. Of particular interest, however, were two small earthquakes that occurred in northeastern Ohio in 1983. The first occurred on 22 January and had a magnitude $m_{bLg} = 2.7$ (NEIC). It was reported by John Carroll University, as well as by stations near Anna and in western Ontario. Its location is rather uncertain (Figure 1); nevertheless, the best estimate of its epicentral position (41.77°N, 81.11°W; Weston Geophysical, 1986) places the earthquake less than 5 km from one of the major injection wells and within 5 km of the Perry Nuclear Power Plant. On 19 November 1983, another earthquake of about magnitude 2.5 was also observed by stations operated by the University of Western Ontario (Weston Geophysical, 1986). Its position is also poorly known, however, because its seismogram is similar in many respects to the January 1983 event; its location is believed to be nearly the same. Its absence from various earthquake catalogs in the United States implies a detection threshold for this part of Ohio prior to the 31 January earthquake of at least magnitude 2.5 or greater.

Main shock

The earthquake of 31 January 1986 occurred at 16:46 UTC. There was no immediate foreshock sufficiently large to record on the instruments at John Carroll University. The main shock was felt over a wide area and as far away as Washington, D.C. The magnitude of the event was $m_b = 5.0$ (NEIC, 1986) based primarily on data from Europe, or $m_{bLg} = 5.0$ (SLU) from surface waves.

The main shock epicenter was located at 41.650°N latitude and 81.162°W longi-

tude (Figure 1), using *P*-wave arrivals from 41 stations (J. Dewey, written communication, 1986). The focal depth was held fixed at 2 km, owing to the lack of depth control and because hypocentral solutions from earlier iterations tended toward negative focal depths. All of the stations used in the location procedure were within 10° of the earthquake, the closest station being CLE (John Carroll University) at 0.32°, and the farthest was POW (Powhatan, Arkansas, SLU) at 9.55°. The velocity model was the same as that developed by Nuttli *et al.* (1969) from earthquake travel times in the Central United States and resulted in a maximum horizontal standard error in location of ±4.6 km at the 90 per cent confidence level.

Within the resolution of the data, the scalar moment of the main shock is estimated to be between 1 and 3 × 10^{23} dyne-cm (M_w = 4.6 to 4.9), based on an inversion of regional surface waves, with a centroid focal depth between 4 to 6 km, and a focal mechanism that is either right-slip (N22°E) or left-slip (N115°E) on nearly vertical nodal planes (Dziewonski, 1986; NEIC, 1986; Herrmann and Nguyen, 1986). Figure 2 shows two possible double-couple components of the moment-tensor solution (small circles), as well as the teleseismic first-motion data (large circle). The focal mechanism solution using only the first-motion data indicates nodal planes oriented at N55°E and N32°W (R. Needham, NEIC, 1986) or about 35° clockwise from those of the moment tensor solutions. Both results, however, exhibit a small component of reverse-slip. Whether this discrepancy in the strike of the nodal planes is the result of incorrect first motions, poor resolution of the surface-wave inversion or possible fundamental differences beween the long- and short-period characters of the earthquake's seismogram is uncertain.

Both the U.S. Geological Survey and Weston Geophysical Corporation conducted intensity studies immediately following the main shock (Wesson and Nicholson, 1986; Weston Geophysical, 1986). Some of the highest intensities found (Modified

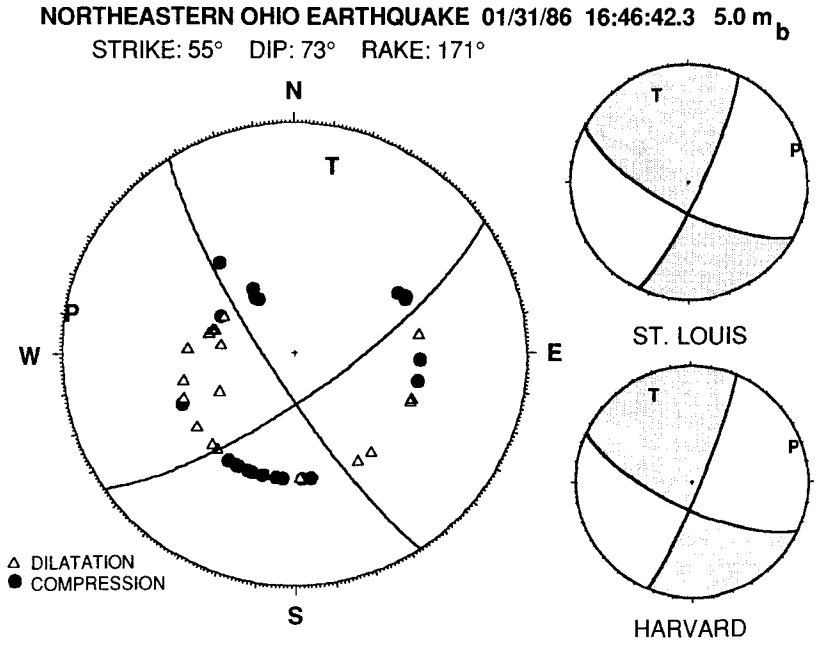

FIG. 2. Focal mechanism solutions of the 31 January main shock from short-period teleseismic first motions (large circle, R. Needham, NEIC, 1986) and from inversion of near-regional surface waves (small cirlces) (SLU = Herrmann and Nguyen, 1986; HARVARD = NEIC, 1986).

Mercalli intensity VI–VII) occurred up to 15 km away from the instrumental epicenter. Damage consisted primarily of broken windows, damaged chimneys, cracks in the walls and foundations, fallen ceiling tiles, items thrown off shelves, and broken gas and water mains. The city sewage lagoon in Chardon sustained considerable damage, and a large area of disturbed water wells was found to extend from southwest of Chardon northeast to Thompson (Figure 3). Seventeen people were treated for minor injuries. Isolated intensities reached VII, although in general the maximum intensity was VI. The intensity at the Perry Nuclear Power Plant was V.

Response of shallow water wells. Reports were obtained from 12 wells, indicating an increase or decrease in water level, water pressure, or flow rate following the main shock (Geauga County Disaster Services Agency, written communication, 1986; Calhio Chemical Company, written communication, 1986; interviews with residents, 1986). In one well close to the epicenter (A, Figure 3), the water level rose by nearly 1.5 m and was sustained at that height for nearly 48 hr. Interestingly, the pattern of these changes is consistent with the pattern of compressions and dilatations predicted for the coseismic volume strain change associated with the main shock. Similar agreement between changes in wells and coseismic volume strain change associated with fault slip has been reported by Wakita (1975) and Roeloffs and Bredehoeft (1985), although many examples exist in which observed

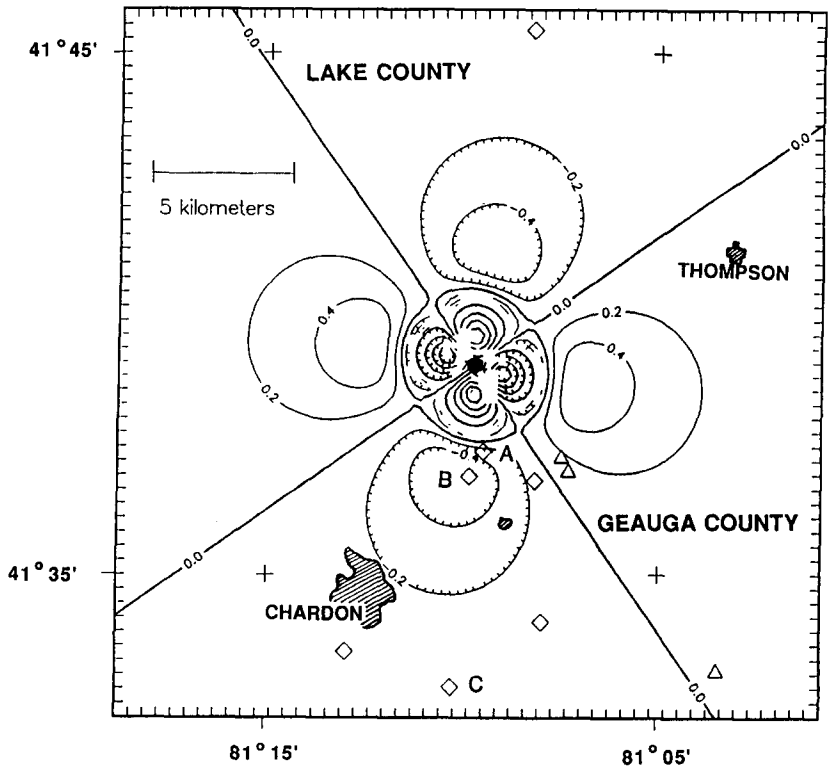

FIG. 3. Volume strain produced by 22 cm of right-slip over a 1.5-km-long vertical fault, oriented N55°E, extending from 1 to 3 km in depth, and centered below the main shock epicenter (solid hexagon). Contour interval is 0.2 μstrain; extension is positive, and compression is negative. Diamonds are sites of water level rise, and triangles are sites of water level fall. Sites indicated by A, B, and C are discussed in the text.

coseismic changes in water level are too large, or of incorrect sign, to reconcile with the predicted volume strains produced by earthquake faulting (e.g., Vorhis, 1968).

In Figure 3, the locations of water level (or pressure or flow) increases, and decreases are superimposed on a plot of the volume strain produced by slip on a fault consistent with the first-motion focal mechanism and seismic moment of the main shock. The calculation assumes 22 cm of slip on a vertical, right-lateral fault 1.5 km long, extending from 1 to 3 km in depth, oriented N55°E, and centered beneath the epicenter of the 31 January earthquake. All 10 observations of changes in water level are consistent with the predicted sign of coseismic volume strain.

Note that for faulting that does not reach the surface, each major quadrant contains a small region in which the volume strain is of opposite sign. The radius of this reversed region increases with the depth to the top of the ruptured area. If the top of the fault that slipped is placed at a depth of 2 km, instead of 1 km, then the sign of the observed water level changes at two wells just south of the main shock (A and B, Figure 3) would be in disagreement. Therefore, the observed water level changes would suggest that faulting during the main shock may have propagated to within 1 km of the surface.

Despite the agreement between the sign of the observed and predicted changes in the wells, the observed amplitudes are much larger than would be expected from such artesian water wells and the size of the earthquake. A given comprehensive volume strain ($\Delta\epsilon$), applied to a confined saturated aquifer, will produce a water level rise (Δh) given by: $\Delta h = (BK_r/\rho_w g)\Delta\epsilon$, where B is Skempton's coefficient, K_r is the bulk modulus of the undrained reservoir rock, ρ_w is the density of water, and g is the acceleration of gravity (Rice and Cleary, 1976; Roeloffs, 1987). This equation predicts a maximum water level change of 10 to 50 cm/μstrain, if B is 1.0 and K_r ranges from 10 to 100 kbars, typical of the type of rock forming the Sharon Conglomerate into which most of the shallow surface wells penetrate. At the two sites where the size of the water level change was reported (A and C, Figure 3), the water level rose by 1.5 and 0.6 m, respectively. However, both wells are located in a region where the inferred volume strain was on the order of 0.2 μstrain or less, corresponding to an expected water level change of only 2 to 20 cm. It is, therefore, difficult to assign much quantitative weight to the water well observations; but if taken qualitatively, then the spatial pattern of water level changes identify 3 of the 4 major quadrants of volume strain produced by a strike-slip earthquake.

Aftershock data and analysis

The analysis of the aftershock sequence covers the period 31 January to 15 April 1986 and includes data collected by the U.S. Geological Survey, as well as the analysis of arrival time and first-motion data obtained from the other cooperating groups, including: Lamont-Doherty Geological Observatory, St. Louis University, Tennessee Earthquake Information Center, University of Michigan, Weston Geophysical Corporation, and Woodward-Clyde Consultants. Most of the instrumentation deployed consisted of single-component, high-frequency analog recorders (e.g., *MEQ* – 800's). There were, however, 10 broadband, wide-dynamic range digital GEOS instruments (Borcherdt *et al.*, 1985) deployed with internal clocks synchronized to radio time code. These stations started operation on 1 February, and several were still in operation as of 3 April. Station locations, time histories, Fourier amplitude spectra, as well as discussions of the deployment and instrument capabilities of the GEOS stations, are given in Borcherdt (1986). A more complete listing of station names, affiliations, and locations for the sites occupied during the

aftershock study is given in Table 1. A map of most of the 64 sites occupied by the various stations deployed is shown in Figure 4.

The velocity model used to locate the earthquakes is given in Table 2. It is a composite from several different sources and consists of five sedimentary layers over crystalline basement at a depth of 2.1 km. The velocity interfaces chosen are

TABLE 1

STATION LOCATIONS DEPLOYED TO MONITOR AFTERSHOCKS THROUGH 15 APRIL 1986

Station Code	Latitude (deg min)	Longitude (deg min)	Affiliation Code*	Dates of Occupation
CON	41N42.06	81W12.55	LDGO	1 Feb.–28 Feb.
GAR	41N47.30	81W10.64	LDGO	1 Feb.–2 Feb.
HLH	41N41.20	81W07.01	LDGO	1 Feb.–28 Feb.
HPV	41N44.41	81W03.08	LDGO	1 Feb.–2 Feb.
HSE	41N33.77	81W06.76	LDGO	2 Feb.–28 Feb.
POP	41N37.23	81W07.05	LDGO	3 Feb.–28 Feb.
TTR	41N35.25	81W11.69	LDGO	2 Feb.–28 Feb.
WKR	41N36.06	81W03.13	LDGO	2 Feb.–2 Feb.
HSOH	41N35.66	81W07.84	Michigan	1 Feb.–2 Feb.
MTOH	41N36.68	81W03.07	Michigan	1 Feb.–2 Feb.
CHOH	41N35.56	81W11.84	SLU	31 Jan.–3 Feb.
HAOH	41N36.46	81W08.51	SLU	31 Jan.–3 Feb.
PAOH	41N45.41	81W11.95	SLU	31 Jan.–3 Feb.
CALM	41N34.1	81W10.3	TEIC	2 Feb.–7 Feb.
ELFM	41N36.8	81W10.9	TEIC	3 Feb.–7 Feb.
FARM	41N38.3	81W10.4	TEIC	2 Feb.–7 Feb.
HOWM	41N35.0	81W07.9	TEIC	1 Feb.–7 Feb.
MONM	41N36.7	81W02.9	TEIC	1 Feb.–7 Feb.
BUR	41N39.24	81W04.94	USGS (Denver)	2 Feb.–11 Feb.
CAL	41N41.21	81W08.89	USGS (Denver)	2 Feb.–11 Feb.
COT	41N34.73	81W05.93	USGS (Denver)	2 Feb.–11 Feb.
CUY	41N33.56	81W10.15	USGS (Denver)	3 Feb.–11 Feb.
ERJ	41N39.44	81W05.00	USGS (Denver)	6 Feb.–11 Feb.
FOT	41N38.90	80W59.69	USGS (Denver)	4 Feb.–11 Feb.
HAM	41N36.18	81W08.48	USGS (Denver)	2 Feb.–11 Feb.
HAR	41N36.67	80W59.62	USGS (Denver)	2 Feb.–4 Feb.
HWK	41N41.83	80W59.03	USGS (Denver)	2 Feb.–11 Feb.
LOX	41N44.58	81W02.60	USGS (Denver)	2 Feb.–11 Feb.
MON	41N35.52	81W02.39	USGS (Denver)	2 Feb.–11 Feb.
WSH	41N37.61	81W13.30	USGS (Denver)	2 Feb.–11 Feb.
GS01	41N48.27	81W08.52	USGS (Menlo Park)	1 Feb.–3 Apr.
GS02	41N43.75	81W09.47	USGS (Menlo Park)	1 Feb.–3 Apr.
GS03	41N39.45	81W10.07	USGS (Menlo Park)	1 Feb.–3 Apr.
GS04	41N36.85	81W17.55	USGS (Menlo Park)	1 Feb.–11 Feb.
GS05	41N35.64	81W08.19	USGS (Menlo Park)	1 Feb.–4 Feb.
GS06	41N37.75	81W03.77	USGS (Menlo Park)	1 Feb.–3 Apr.
GS07	41N32.40	81W04.26	USGS (Menlo Park)	1 Feb.–11 Feb.
GS08	41N32.38	81W12.93	USGS (Menlo Park)	2 Feb.–10 Feb.
GS09	41N24.81	81W11.91	USGS (Menlo Park)	2 Feb.–10 Feb.
GS11	41N09.20	81W04.42	USGS (Menlo Park)	2 Feb.–10 Feb.

* LDGO = Lamont-Doherty Geological Observatory, Columbia University; Michigan = University of Michigan; SLU = St. Louis University; TEIC = Tennessee Earthquake Information Center; USGS = U.S. Geological Survey; Weston Geophysical = Weston Geophysical Corporation; Woodward-Clyde = Woodward-Clyde Consultants.

TABLE 1—*Continued*

Station Code	Latitude (deg min)	Longitude (deg min)	Affiliation Code*	Dates of Occupation
GS55	41N37.10	81W07.18	USGS (Menlo Park)	4 Feb.–10 Feb.
CFD	41N40.45	81W13.41	Weston Geophysical	4 Feb.–15 Apr.
CLD	41N31.44	81W20.19	Weston Geophysical	1 Feb.–20 Feb.
HTG	41N37.17	80W57.27	Weston Geophysical	1 Feb.–8 Apr.
KEL	41N32.82	81W06.12	Weston Geophysical	20 Feb.–15 Apr.
MFD	41N27.77	81W04.41	Weston Geophysical	1 Feb.–14 Feb.
MIN	41N33.56	81W15.41	Weston Geophysical	1 Feb.–1 Mar.
PAT	41N33.63	81W21.91	Weston Geophysical	1 Mar.–15 Apr.
PER	41N48.06	81W08.61	Weston Geophysical	1 Feb.–15 Apr.
TOM	41N41.29	81W03.09	Weston Geophysical	2 Feb.–15 Apr.
WEL	41N45.00	81W09.31	Weston Geophysical	24 Feb.–15 Apr.
WC01	41N36.90	81W18.08	Woodward-Clyde	31 Jan.–15 Apr.
WC02	41N40.05	81W09.53	Woodward-Clyde	1 Feb.–15 Apr.
WC03	41N43.87	81W04.46	Woodward-Clyde	1 Feb.–14 Apr.
WC04	41N35.10	81W09.36	Woodward-Clyde	1 Feb.–22 Feb.
WC06	41N32.40	81W01.75	Woodward-Clyde	1 Feb.–14 Apr.
WC07	41N48.00	81W08.58	Woodward-Clyde	3 Feb.–24 Feb.
WC08	41N40.24	81W14.48	Woodward-Clyde	6 Feb.–25 Mar.
WC09	41N35.45	81W09.36	Woodward-Clyde	23 Feb.–14 Apr.
WC10	41N40.04	81W14.45	Woodward-Clyde	27 Mar.–14 Apr.

TABLE 2

VELOCITY MODEL USED TO LOCATE EVENTS LISTED IN TABLE 3

Depth (km)	Thickness (km)	*P* Velocity (km/sec)	*S* Velocity (km/sec)	V_p/V_s	Description*
0.0	0.05	1.80	0.60	3.00	Glacial till
0.05	0.45	3.00	1.58	1.90	Devonian shale
0.50	0.50	4.20	2.33	1.80	Silurian dolomite
1.00	0.75	4.50	2.53	1.78	Ordovician limestone and dolomite
1.75	0.35	4.75	2.70	1.76	Cambrian sandstone and dolomite
2.10	17.90	6.15	3.54	1.74	Precambrian granite
20.00	20.00	6.70	3.87	1.73	Lower crust
40.00	99.00	8.15	4.63	1.75	Mantle

* Cleveland Electric Illuminating Co. (1982).

based on extensive regional compilations of well data drilled at least as far as the top of the Precambrian basement (Cleveland Electric Illuminating Co., 1982). An average of down-hole and cross-hole velocity logs is used to determine the *P*- and *S*-wave velocities in the upper 0.5 km. Velocities in the basement, lower crust, and mantle are based on the same regional velocity model as was used to locate the main shock (i.e., Nuttli *et al.*, 1969). Velocities in the Paleozoic section are inferred from refraction studies in adjacent areas (Press, 1966). This model is not locally well constrained. With the exception of the near-surface *P* and *S* velocities, the velocities used are not based on actual *in situ* measurements in the epicentral region. Furthermore, this model does not take into consideration the very slight dip of the top of the Precambrian interface, which near the shore of Lake Erie is about 1830 m (6,000 feet) deep but near the epicentral region, it is about 2130 m (7,000 feet).

As a test of the location process, several different velocity models were tried, including a simple layer over a half-space to accommodate the slower Paleozoic section over granitic basement (Wesson and Nicholson, 1986). Owing to the excellent station coverage, however, it was apparent that regardless of the velocity model

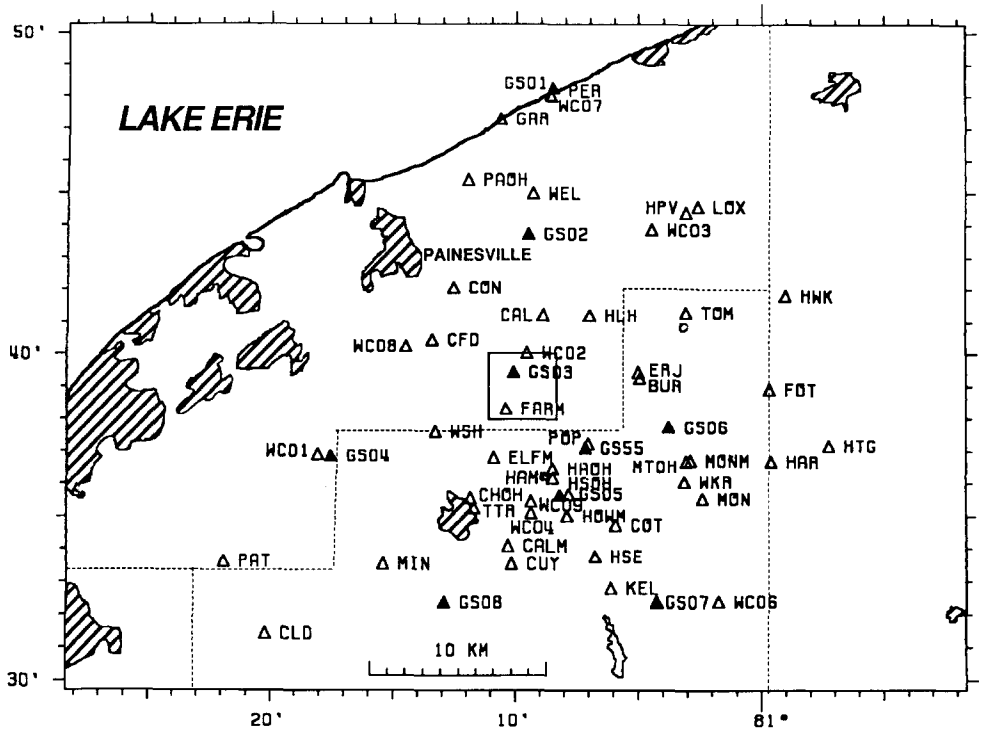

FIG. 4. Seismograph stations deployed by all cooperating institutions to record aftershocks of the January main shock (large square). Solid symbols are digital recording sites. *Shaded areas* on this and subsequent maps represent areas of dense population. Dashed lines are county boundaries.

tried, the earthquake epicenters did not vary by more than about 0.5 km. Only the focal depths were significantly affected, with systematic biases of up to 1 km observed between the various velocity models used.

The earthquakes were located using HYPOELLIPSE (Lahr, 1985) and as many of the available arrival times as were internally consistent. Arrivals based on the digitally recorded GEOS instruments were given preferential weight because of the higher precision of timing, the greater resolution in picking the arrivals, and the greater confidence in identifying the shear-wave arrival on the three-component instruments. A serious complication was that many of the single-component stations reported secondary arrivals that were often a converted phase (e.g., S to P). Thus, in order not to mix both converted and direct shear arrivals, only S arrivals from the GEOS three-component stations were used. However, all of the available P-wave data were included, permitting better station coverage and therefore greater precision and azimuthal control.

Aftershock locations

As of 15 April, 13 aftershocks were located (Figure 5). Most of these events occurred within the first 8 days; two were felt. Coda magnitudes ranged from 0.5 to 2.5, based on a formula developed for earthquakes in the Central United States (Stauder *et al.*, 1981). These values match other magnitudes derived from scalar moments determined from the GEOS digital recordings, assuming the largest aftershock is equivalent to a magnitude 2.4 (see Table 3; Glassmoyer *et al.*, 1986; Borcherdt and Glassmoyer, 1987). In addition to the aftershocks, several events

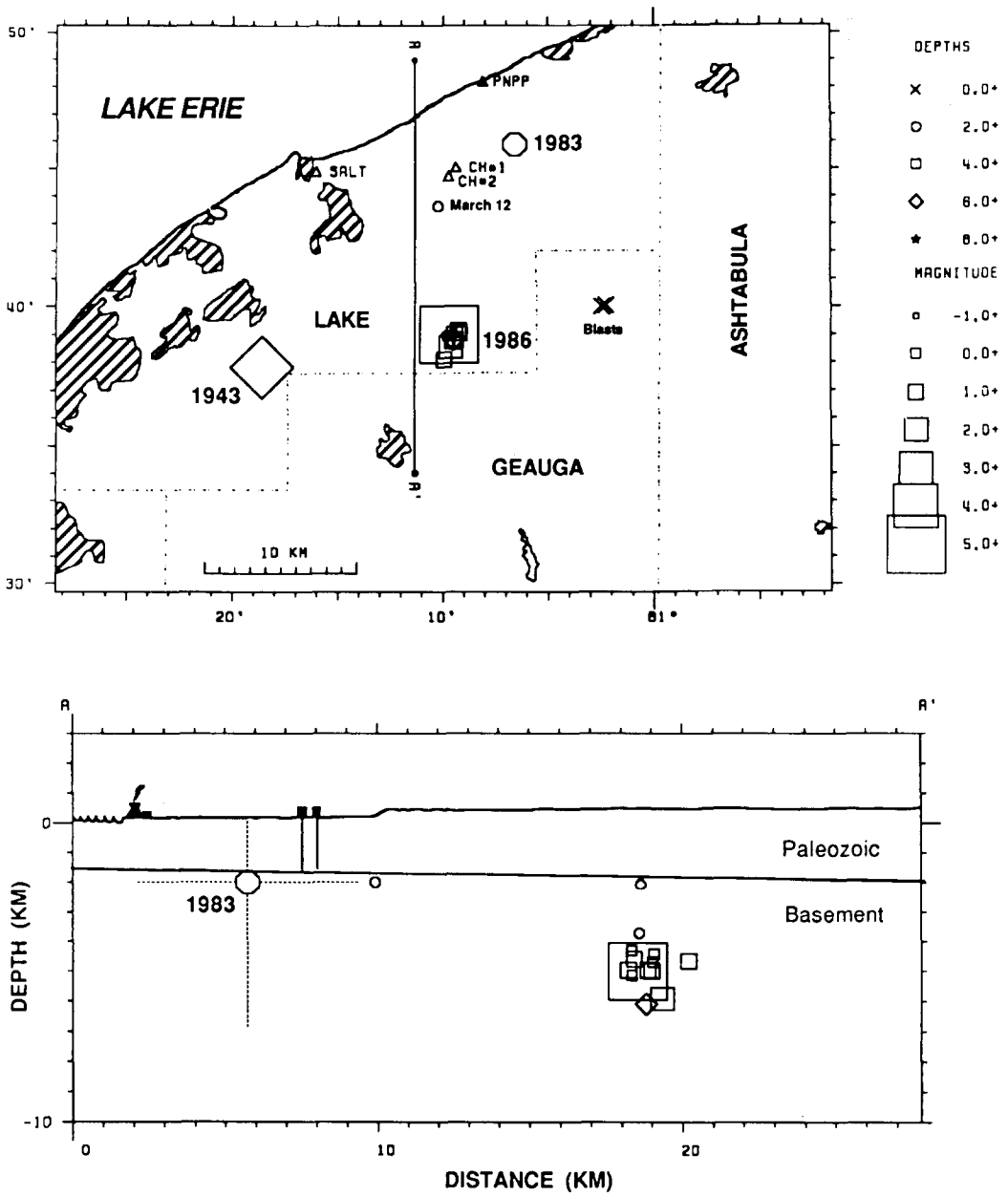

FIG. 5. (*Top*) Location of deep injection wells and recent earthquake epicenters in northeastern Ohio as of 15 April 1986. Large uncertainties in location are associated with both the 1943 and 1983 earthquake epicenters. Local quarry blasts are shown as crosses. CH#1 and CH#2 (Calhio #1 and Calhio #2) are the deep waste disposal wells; SALT is the Painesville brine well. (*Bottom*) Vertical cross-section, no exaggeration, along the line *A–A'* shown above. Main shock focal depth corresponds with mean centroid depth.

believed to be quarry blasts were also recorded (Figure 5). Because of the dense network of stations (Figure 4), location accuracy for all of the events detected was on the order of 0.5 km at the 90 per cent confidence level, with even the smallest event being recorded by at least six stations.

Figure 6 shows the aftershock locations as well as station coverage within the

TABLE 3

LOCATIONS OF RECENT EARTHQUAKES AND BLASTS IN NORTHEASTERN OHIO

Date (YrMoDy)	Origin (Hr:Mn Sec)	Latitude (deg min)	Longitude (deg min)	Depth (km)	Magnitude	No. PHA	rms (sec)	ERH (km)	ERZ (km)	Azimuth Gap
				Main Shock and Prior Events						
430309	03:25 25.00	41N37.80	81W18.60	6.50	4.7	14	1.45	11.9	16.8	206
830122	07:46 57.80	41N45.90	81W 6.60	2.00*	2.7	18	0.38	4.20	5.80	92
860131	16:46 42.30	41N39.00	81W 9.72	2.00*	5.0	41	0.75	4.60	—	58
				Aftershocks						
860201	18:54 49.20	41N38.82	81W 9.42	4.97	1.5	21	0.13	0.80	1.66	100
860202	3:22 48.53	41N38.75	81W 9.53	4.99	1.2	24	0.06	0.25	0.57	72
860203	19:47 19.61	41N38.84	81W 9.50	6.10	1.9	44	0.10	0.33	0.68	73
860205	6:34 2.40	41N38.94	81W 9.64	2.07	0.9	20	0.21	0.83	0.98	49
860206	18:36 22.24	41N38.56	81W 9.64	5.92	2.4	43	0.12	0.39	0.82	48
860207	15:20 20.20	41N39.06	81W 9.24	4.59	1.4	27	0.08	0.29	1.06	42
860210	20:06 13.49	41N39.16	81W 9.27	4.97	1.3	26	0.09	0.42	1.16	69
860223	3:29 48.41	41N39.10	81W 9.30	5.13	0.9	23	0.09	0.39	1.17	73
860224	16:55 6.37	41N38.96	81W 9.81	3.72	0.8	10	0.09	0.71	3.32	126
860228	1:39 34.07	41N39.11	81W 9.59	4.31	0.8	12	0.08	0.69	1.66	92
860308	20:42 49.48	41N38.71	81W 9.31	4.42	0.9	20	0.10	0.46	1.37	103
860312	8:55 26.59	41N43.64	81W10.25	2.00	0.7	10	0.06	1.35	0.78	216
860324	13:42 41.22	41N38.10	81W 9.95	4.66	1.5	16	0.10	0.53	1.56	88
860410	6:58 5.59	41N38.74	81W 9.67	4.69	0.8	22	0.09	0.36	0.86	65
				Blasts						
860205	15:39 6.45	41N40.08	81W 2.28	0.90	1.1	13	0.09	1.30	1.24	74
860205	17:57 3.85	41N40.02	81W 2.46	0.01	1.0	12	0.07	0.46	0.74	75

Magnitudes, Moments, and Focal Mechanisms

Date (YrMoDy)	Origin (Hr:Mn Sec)	Magnitude N.E.†	Magnitude N.M.‡	Moment (dyne-cm)	Magnitude§ (M_w)	N/NE Slip Plane			*P* Axis	
						Strike	Dip	Slip	Azimuth	Plunge
860131	16:46 42.30			(first-motion data)		55	73	171	280.4	5.8
	(centroid depth: 4–6 km)			1-3E+23	4.6	22	81	160	69.6	7.3
860201	18:54 49.20	1.5	1.5			30	70	169	72.0	6.6
860202	3:22 48.53	0.9	1.2	2.0E+18	1.1	70	75	160	293.3	2.9
860203	19:47 19.61	2.0	1.9	21.3E+18	2.1	45	82	140	273.3	21.1
860205	6:34 2.40	0.1	0.9	1.3E+18	0.9	195	90	165	61.0	10.5
860206	18:36 22.24	2.5	2.4	38.8E+18	2.4	30	90	165	256.0	10.5
860207	15:20 20.20	1.1	1.4	8.0E+18	1.6	5	70	169	47.0	6.6
860210	20: 6 13.49	1.0	1.3	4.6E+18	1.5	180	80	−170	45.9	14.1
860223	3:29 48.41	0.1	0.9	1.0E+18	0.8	7	80	170	50.9	0.1
860224	16:55 6.37	−0.1	0.8							
860228	1:39 34.07	−0.1	0.8							
860308	20:42 49.48	0.1	0.9			2	70	160	43.4	0.8
860312	8:55 26.59	−0.3	0.7	0.8E+18	0.7					
860324	13:42 41.22	1.4	1.5			195	85	−180	59.9	3.5
860410	6:58 5.59	−0.1	0.8			25	81	150	250.9	14.3

* Fixed depth.

† New England coda-magnitude formula ($M_c = 2.2 \log D - 1.7$) (Chaplin *et al.*, 1980).

‡ New Madrid coda-magnitude formula ($M_c = 2.7 \log D - 2.7$, $D \geqq 40$ sec; $M_c = 0.9 \log D + 0.2$, $D <$ 40 sec) (Stauder *et al.*, 1981).

§ Moment magnitude ($M_w = \log M_0 - 17.2$, $M_w < 2.5$; $M_w = 0.67 \log M_0 - 10.7$, $M_w \geqq 2.5$).

immediate vicinity of the main shock. Although most of the aftershock activity remains in a very small cluster, there was one event on 24 March that is located about 1 km outside the immediate source region of the main shock. Its location to the south-southwest, coupled with a poorly resolved trend in the earthquake

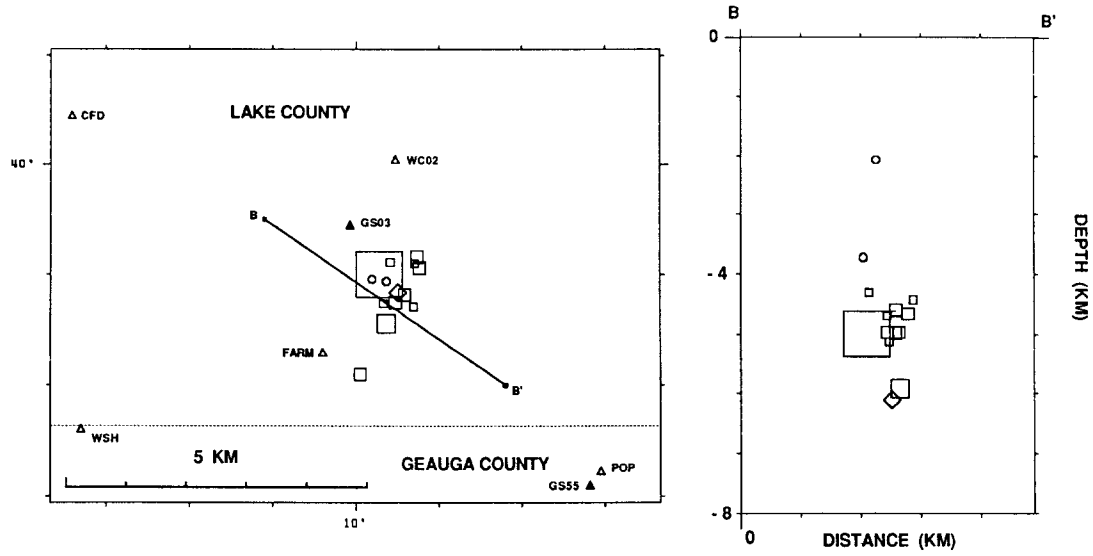

FIG. 6. (*Left*) Map of aftershock locations within the immediate epicentral region of the main shock. (*Right*) Vertical cross-section perpendicular to N30°E.

epicenters, suggests a short fault segment oriented 25° to 35° east of north, or close to one of the nodal planes observed in the focal mechanism solution of the main shock. A vertical cross-section taken perpendicular to a strike of N30°E (right, Figure 6) is consistent with rupture initiating at depth on a nearly vertical fault with a north-northeast orientation.

In addition to the tight cluster of aftershocks, one small earthquake (M_c = 0.7) was detected near station GS02 (Figure 5) on 12 March. The seismogram as recorded on the GEOS instrument (GS02) is shown in Figure 7. Its location based on arrivals at GS02 and the Woodward-Clyde stations is 41.727°N, 81.170°W, with a focal depth of 2.0 km. The correspondence of this hypocenter with the base of the Paleozoic section and its relative proximity to two of the deep injection wells in Lake County (less than 3 km) suggest that this single event may have been triggered by adjacent injection activities. It should be noted that similar earthquakes of this size would not have been detected prior to the occurrence of the 31 January earthquake and the subsequent deployment of sensitive seismographic equipment in the epicentral region.

Focal mechanism solutions

Single-event focal mechanism solutions (lower hemisphere, equal-area projections) were constructed using polarity data from nearly all of the temporary stations deployed (Figure 8). Nodal planes were determined using the grid searching program FPFIT (Reasenberg and Oppenheimer, 1985). Two general classes of focal mechanism solutions were observed. The first type of solution (Figure 8A) exhibited nodal planes oriented northeast and northwest. The *P* axis is nearly horizontal and varies from east-northeast to east. This class includes the two largest aftershocks and therefore represents some of the best-constrained results. The northeast-striking nodal plane is consistent with the general distribution of the aftershock hypocenters (Figure 6) and would typically be assumed to represent the actual plane of faulting. If so, then motion during the earthquakes would have been predominantly oblique right-slip on a nearly vertical fault.

The second class of focal mechanism solutions (Figure 8B), although somewhat

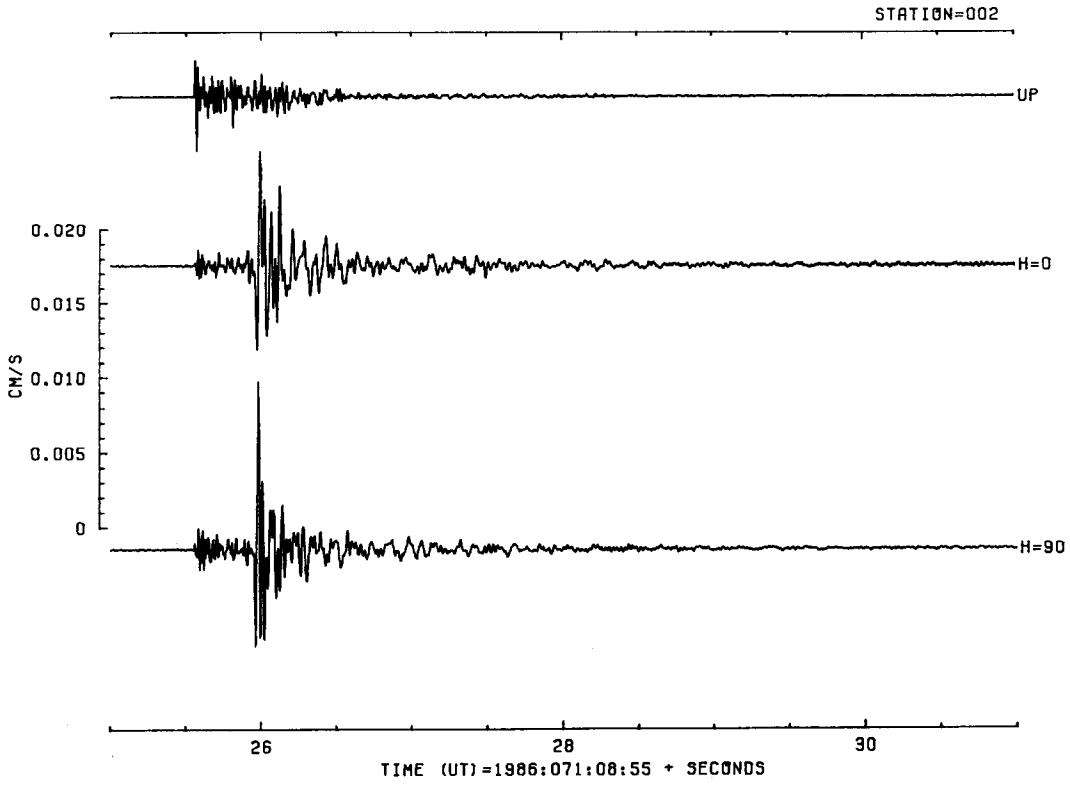

FIG. 7. Seismogram of small event on 12 March near station GS02 within 3 km of the Calhio injection wells (courtesy of R. Borcherdt, C. Mueller, and G. Glassmoyer). See Figure 5 for location.

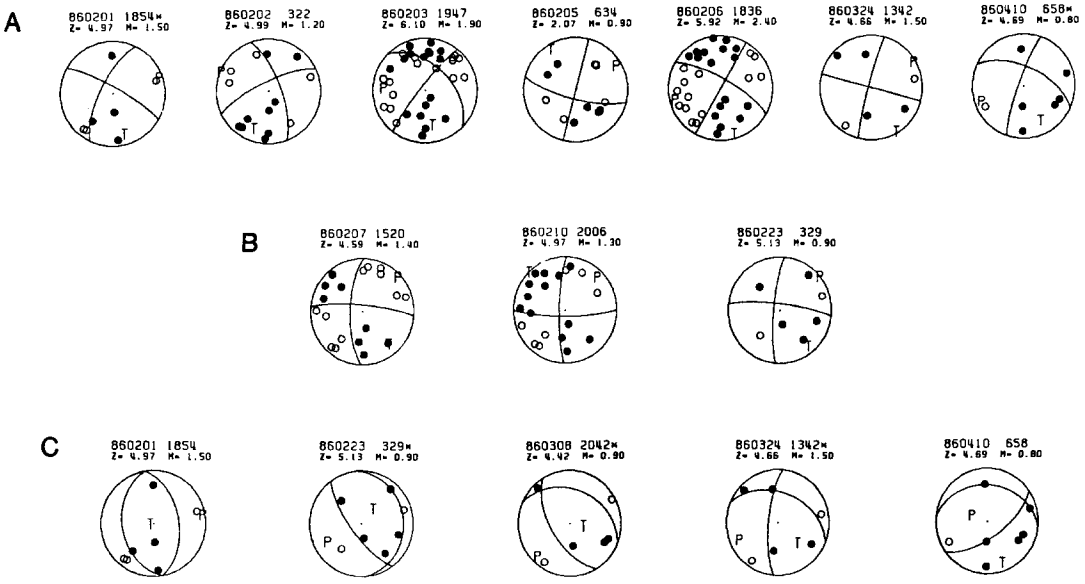

FIG. 8. Lower hemisphere, equal-area, single-event focal mechanisms determined using a grid search for nodal planes. (A) Oblique-slip focal mechanisms with a nodal plane oriented north-northeast–northeast. (B) Nearly pure strike-slip mechanisms with a nodal plane oriented north-south. (C) Alternative solutions for poorly constrained focal mechanisms. Solid circles are compressions, and open circles are dilatations. Legend indicates origin time, focal depth, and magnitude.

less well resolved, exhibits a nodal plane oriented nearly north-south and a P axis oriented more toward the northeast. This observation of different focal mechanisms found within a single aftershock sequence is not unusual and suggests that more than one favorably oriented, weak fracture is being reactivated by the change in stress associated with the main shock. Several of the smaller earthquakes also permit alternative focal mechanism solutions with large dip-slip components (Figure 8C). These alternate solutions are considered unlikely, primarily because of the predominance of the nearly strike-slip mechanisms exhibited by the better-constrained results.

Relation to regional tectonics

In general, most of the focal mechanisms are consistent with a horizontal maximum compressive stress field striking northeast to east, consistent with the P axis determined from the main shock (Figure 2) and regional determinations of stress orientation for the Central United States (e.g., Zoback and Zoback, 1980). Furthermore, because the aftershock slip orientations vary from predominantly strike-slip to oblique slip with typically 10° of rake or less, this implies that the vertical stress is probably the intermediate principal stress.

All of the earthquakes occurred at or below a depth of 2 km, corresponding to the interface of the Paleozoic section with the Precambrian granitic basement. In common with other earthquakes in the Eastern United States, no surface manifestation of the active fault plane has yet been found. The earthquakes occurred on the western flank of the Appalachian Basin, within which rocks of Paleozoic age dip monotonically to the east and southeast away from the axis of the Cincinnati Arch in western Ohio. Basement rocks, however, are an extension of the Grenville Province that forms the eastern section of the Canadian shield. Although this area of Ohio has been extensively surveyed and drilled, primarily for natural gas and salt explorations, few investigations penetrated to the crystalline basement. Regional gravity and magnetic studies, however, suggest the presence of several large-scale basement structures, one of which defines a northeast-striking lineation. This line consists of a series of magnetic highs separating a region of low magnetic relief to the southeast from an area of high magnetic relief to the northwest (Hildenbrand and Kucks, 1984a; Weston Geophysical, 1986). Moreover, the Bouguer gravity anomaly map shows an odd-shaped high centered over much of Lake County (Hildenbrand and Kucks, 1984b) that could reflect an area of higher density basement material offset in a right-lateral sense across a zone that has nearly the same strike as the ridge defined by the line of magnetic highs. This line is coincident with the location of the main shock and the distribution of aftershocks, and has a regional strike of about N40°E. Most recognized subsurface faults, or other basement structures, however, typically trend northwest or west-northwest (e.g., Root and MacWilliams, 1986), similar in orientation to many of the auxiliary nodal planes observed in the earthquake focal mechanisms (Figure 8A).

Fluid Injection in Northeastern Ohio

Previous examples of earthquakes and injection well activities

It has been conclusively demonstrated that under some conditions, the increase in fluid pressure in the earth's crust as the result of the injection of fluid can tigger earthquakes (c.f. Raleigh *et al.*, 1976). In each of the well-documented examples, convincing arguments that the earthquakes were induced relied upon three principal characteristics of the subsequent earthquake activity. First, there is a very close

geographic association between the zone of increased fluid pressure and the locations of the earthquakes in the resulting sequence. Second, calculations based on the measured or inferred state of stress in the earth's crust, and the measured injection pressure, indicate that the theoretical threshold for frictional sliding along favorably oriented, preexisting fractures was likely exceeded. Third, a clear disparity between the previous seismicity and the subsequent earthquake activity could be established, with the induced seismicity often characterized by large numbers of small earthquakes that persisted for as long as elevated pore pressures in the hypocentral region continued to exist. Two of the best documented cases for induced seismicity are summarized below, because they bear directly on whether the Ohio earthquake may be considered induced, and to illustrate the quality of the evidence for previous examples of seismicity related to fluid injection.

In 1962, at the Rocky Mountain Arsenal near Denver, Colorado, the injection of 17 to 21 million liters/month of waste in to a 3671 m deep disposal well was quickly followed by many felt earthquakes in a region where the last felt earthquake had occurred in 1882 (Healy *et al.*, 1968). A study of event locations showed that the earthquakes were occurring in an elongate region about 10 km long and 3 km wide, centered on the well and at depths of 4 to 7 km. A comparison of earthquake frequency and average injection rate showed a convincing correlation. Although injection was stopped in February 1966, earthquakes continued to occur, not near the base of the well, but primarily within the previously defined linear zone and at a distance of 4 to 6 km. The largest earthquakes in the sequence (between 5 and 5.5) occurred in April, August, and November 1967, after which activity began to decline. Hsieh and Bredehoeft (1981) demonstrated that the records of pressure falloff at the disposal well were consistent with injection into a long, narrow reservoir; a conclusion supported by the elongate shape of the seismogenic zone. Based on their model, a fluid pressure increase of 32 bars was apparently sufficient to trigger seismic activity along favorably oriented, preexisting fractures. No hydraulic stress measurements were ever made near the Rocky Mountain Arsenal. Healy *et al.* (1968) inferred a least compressive stress of 362 bars at the bottom of the disposal well from the pressure at which the volume rate of injection increased rapidly, and estimated a maximum compressive stress to be at least the overburden pressure of 830 bars. The estimated formation pressure prior to injection was 269 bars. With injection pressures at the Rocky Mountain Arsenal having apparently reached a maximum of 72 bars above ambient, fluid pressures within the reservoir were inferred to be capable of initiating failure along favorably oriented fractures with cohesive strengths of as much as 82 to 100 bars.

Solution mining for salt near Dale, New York, triggered a marked increase in microearthquake activity in 1971 (Fletcher and Sykes, 1977). As many as 80 earthquakes/day were concentrated within 1 km of a 426 m deep injection well in an area where the previous record of activity was less than one event/month. Tophole pressure at the injection well typically operated between 52 to 55 bars, or only a few bars less than that calculated to induce sliding on preexisting fractures with no cohesion, based on the analysis of hydrofracture stress measurements conducted about 100 km from the activity. The low level of background seismicity prior to high-pressure injection, the dramatic increase in activity following injection, and the rapid cessation of activity following a decrease in injection pressure below about 50 bars strongly suggested that this seismicity was induced.

These two cases demonstrate that, in sufficiently prestressed regions, elevating formation pore pressure by several tens of bars can cause a previously quiescent

area to become seismically active. Furthermore, although initial seismicity is usually concentrated near the base of the active wells, later seismicity can occur at distances as far away as several kilometers and long after injection has ceased. In the case of the Ohio earthquake of 31 January, both types of injection activities (solution salt mining and high-pressure waste disposal) have occurred or are now in current operation within the northeast region of the state.

Solution salt mining

The association of solution mining with the occurrence of small earthquakes in western New York State (Fletcher and Sykes, 1977), and the extensive salt mining operations in northeastern Ohio (Clifford, 1973), suggested the possibility that some of the recent seismicity in Ohio may be related to solution salt mining. Solution mining for salt began in northeastern Ohio in 1889 (Clifford, 1973; Dunrud and Nevins, 1981) and continues to the present, although several previously active operations have been closed down. The target horizon for the mining operations is the Silurian Salina formation at a depth of 600 to 900 m, depending on distance from Lake Erie. Based on their spatial proximity and temporal association, it could be argued that several earthquakes in the northeast region of the state could be associated with solution salt mining operations active at the time the earthquakes occurred. In particular, earthquakes in 1898, 1906, and 1907 (Stover *et al.*, 1979) located within the Cleveland metropolitan area, as well as earthquakes in 1932, and 1940, about 50 km south of Cleveland (Figure 1), are possible examples. However, in view of the large number of earthquakes reported prior to the initiation of solution mining, and the apparent occurrence of at least some earthquakes in northeastern Ohio beyond the range of expected influence from mining operations, it seems reasonably clear that at least some of the earthquakes are natural and that solution mining is not a necessary condition for the occurrence of earthquake activity. Moreover, the relatively low injection pressures involved (typically less than 50 bars), the shallow depth of the mining operations (less than 1 km and above several impermeable shale layers), and the fact that all solution salt mining operations within Lake County have long since ceased, argue against solution mining having significantly elevated pore pressure in the Precambrian basement, or having triggered the 31 Janauary earthquake.

High-pressure waste disposal operations

Three high-pressure fluid injection wells that penetrate into basement are currently operating within Lake County, Ohio and are within 15 km of the epicentral region of the main shock. One is an oil-field brine disposal well (SALT) located within the Painesville township (Figure 5) in an area where considerable solution salt mining had previously occurred. Total volume of fluid injected into this brine well prior to 31 January 1986 amounted to about 5 million liters at a top hole presure of 55 bars (800 psi) (Ohio Division of Oil and Gas, written communication, 1986). The other two deep injection wells are much more likely candidates for possible earthquake triggering in view of their injection history and length of operation. These two 1800 m deep wells are located near Perry, Ohio (CH#1 and CH#2, Figure 5) and are operated by Calhio Chemicals Division of the Stauffer Chemical Company to dispose of waste products from the manufacture of an agricultural fungicide. The first of these wells, Calhio #1, was completed in 1971 Natural Resources Management Corp., 1971). Full-scale injection of waste into the well began in 1975. A second well, Calhio #2, was completed in 1981 and has been

used as a backup to the first well since that time (Resource Services, Inc., 1980). More than 1.19 billion liters (315 million gallons) of fluid have been injected into the two wells, principally into Calhio #1 (Figure 9) between March 1975 and February 1986 (Ohio EPA, written communication, 1986). Injection pressures at a typical injection rate of 320 liters/min (85 gal/min) have reached a maximum of 112 bars top-hole pressure.

Although the distance from the Calhio wells to the 31 January earthquake (12 km, Figure 5) is greater than the corresponding distances in either the Denver or Dale cases, the total volume of fluid injected into the Calhio wells and the pressures involved are significantly greater. Thus, in order to assess the degree to which fluid injection activities could have influenced earthquake activity in northeastern Ohio, it is necessary to assess the current state of stress at the bottom of the wells and to determine how rapidly the effect of the wells attenuates with distance, by examining the hydrologic properties of the reservoir into which fluid is being injected.

Estimation of the state of stress

The principle sources of information about existing crustal stresses at the bottom of the wells, or in adajcent regions, are: measurements of the instantaneous shut-in pressure (ISIP) made during commercial hydrofracture operations; breakdown pressures measured during well stimulation; fracture reopening pressures; and focal mechanism orientations of nearby earthquakes. In the case of Lake County, Ohio, data from all three injection wells, as well as the recent seismicity, can be used to set bounds on each of the three principal stresses. Estimates on the regional character of the state of stress are available from hydrofracture stress measurements made in Michigan and in western New York (Haimson, 1978; Hickman *et al.*, 1985).

State of stress at bottom of injection wells. Table 4 lists relevant values for principal stresses available from both existing well data and regional compilations. Large uncertainties exist for many of these values (particularly the maximum horizontal compressive stress), mainly because commercial measurements are ill-suited for this analysis and because, in nearly all cases, some assumptions, interpretations, or extrapolations of the existing data had to be made to determine the values calculated. The preferred values listed at the bottom of the table are not simply averages of all available calculations for that particular parameter, but represent our considered opinion as to the most likely estimate.

The vertical stress (S_v) can be calculated once the weight of the overburden is known. Density logs taken in the Calhio wells indicate an average density of 2.6 gm/cm^3 throughout the Paleozoic section (Natural Resources Management, 1971). This implies a gradient of 0.255 bar/m or 460 bars at the bottom of the well. Nearly identical values of overburden stress were measured in a deep Michigan hole drilled through similar materials (Haimson, 1978).

Values for the least horizontal stress (S_h) at the base of the Paleozoic section (bottom of the wells) can be estimated from ISIP recorded while each of the wells was hydrofractured. This measurement is valid if the fractures produced in the wells were vertical and propagated parallel to the maximum horizontal compressive stress. In addition, some uncertainty is introduced in correcting this value to the bottom of the well (BHP) because, although most of the wells were stimulated with fresh water, other material in the injected fluid (acid, sand, salts, etc.) raises its density by an unspecified amount. To simplify matters, a standard value of 180 bars is assumed for the correction to the bottom of the wells (1810 m), unless information was available to indicate a different value was more appropriate. In

TABLE 4

STRESS AND PRESSURE ESTIMATES (IN BARS) AT A DEPTH OF 1.8 KM

Measurement Site*	Principal Stresses			Formation Pore Pressure§		Injection Pressure
	S_v	S_h†	S_H‡	Maynardville	Mt. Simon	
Michigan (Haimson)	464	344	503			
Western New York (Hickman *et al.*)	441	370	570			
Calhio #1 (initial)	461	305	488–514	170	187	
						291
Calhio #1 (final)		340	529–555	194	213	
Calhio #2 (initial)	462	320	463–527	195	199	
						291
Calhio #2 (final)		346	504–567	202	206	
Brine well (initial)	459	271				
						267
Brine well (final)		295				
Adopted value	460	300–320	460–560	200		290

* Measurements made in the Calhio #1 well were conducted on 11 April 1971. Measurements made in the Calhio #2 well were conducted on 20 August 1979. Measurements made in the Brine well (SALT) were conducted on 2 January 1985.

† ISIP.

‡ Derived from fracture breakdown (initial) and fracture reopening (final) pressures using various combinations of pore pressure and ISIP, e.g., $P_{bd} = 3\ (S_v) - S_H - P_0 + T_0$, where P_0 = pore pressure and T_0 = tensile strength.

§ Measured after standard slug test (initial) and upon final equilibrium.

several cases, values for the ISIP are measured both early and late into the hydrofracture procedure. Table 4 lists both measurements. Since measurements made after extended pumping of the materials used in commercial operations often yield an overestimate of the least horizontal stress, initial values of ISIP are assumed to be more appropriate.

Initial values of ISIP corrected to the bottom of the wells range from 271 to 320 bars. Extrapolations from down-hole measurements made at regional distances (Michigan and western New York) range as high as 370 bars (Haimson, 1978; Hickman *et al.*, 1985). The preferred value is taken to be 300 to 320 bars.

Formation pore pressure was measured directly during drill stem tests about 8 yr apart at the two Calhio wells. Table 4 lists values measured just after the standard pump test (initial) and upon reaching equilibrium (final) in both the Mt. Simon and Maynardville formations. Both sets indicate a change in the formation pore pressure as measured in the Calhio #2 well, since extensive pumping began in the Calhio #1 well 4 yr earlier (1975). This apparent increase in pore pressure with time (found predominantly in the Maynardville) is consistent with calculated effects of fluid injection in the adjacent well. In any case, the values obtained are all close to hydrostatic if the density of the connate water is assumed to be 1.2 gm/cm^3 (Table 5).

From the focal mechanism solutions of the earthquakes, the maximum horizontal compressive stress (S_H) is at or above the vertical stress (i.e., $\geqq$460 bars). Based on the previously derived values of S_h and pore pressure, estimates of S_H derived from formation breakdown pressures during well stimulation in the Calhio wells give values that range as low as 463 bars (initial values, Table 4), but they need to be corrected the tensile strength of the rock, revising these estimates upwards from 40 to 100 bars. Estimates of the maximum horizontal compressive stress made from attempts to interpret the pumping records for fracture-reopening pressures are

TABLE 5

PHYSICAL PROPERTIES OF RESERVOIR ROCKS INTO WHICH WASTE IS BEING INJECTED

		Maynardville	Mt. Simon
Depth to top (m)	Calhio #1	1667	1806
	Calhio #2	1672	1811
Permeability (darcies)	Calhio #1	$4.2–5.4 \times 10^{-3}$*	$2.9–5.5 \times 10^{-3}$*
	Calhio #2	2.1×10^{-3}†	5.5×10^{-3}*
Hydraulic conductivity (m/sec)	Calhio #1	4.2×10^{-8}	5.5×10^{-8}
	Calhio #2	2.1×10^{-8}	5.5×10^{-8}
Thickness (m)	Calhio #1	52.7	37.8
	Calhio #2	52.4	35.7
Specific gravity of connate brine	Calhio #1	1.194	1.158
	Calhio #2	1.213	1.143
Transmissivity (m^2/sec)	Calhio #1	2.2×10^{-6}	2.1×10^{-6}
	Calhio #2	1.1×10^{-6}	2.1×10^{-6}
Porosity	Calhio #1	8%*	8.5%†
	Calhio #2	2–4%†	9%‡
Minimum storativity	Calhio #1	1.25×10^{-5}	9.54×10^{-6}
	Calhio #2	6.25×10^{-6}	1.11×10^{-5}

Other values assumed are: density of injected fluid = 1.05 g/cm^3; fluid compressibility = 3.03×10^{-11} cm^2/dyne (Natural Resources Management Corp., 1971; Resources Services, Inc., 1980).

* Drill stem test.

† Core sample.

‡ Well log.

listed in Table 4 as final values. Measurements derived from well records made during the stimulation of the brine well near Painesville are suspect, since the hydrofracture procedure was conducted through perforated casing (Petro Evaluation Services Inc., 1985). Thus, of all the measurements, the value of the maximum compressive stress is the least well known. For our purposes, estimates of the maximum compressive stress based on a lower bound (i.e., the vertical stress of 460 bars) are useful, as they would represent conservative estimates on how close to failure conditions are at the top of the basement.

The Mohr-Coulomb failure criterion. Using the adopted values given in Table 4, it appears that without fluid injection, the conditions are near but do not exceed failure at the bottom of the wells. Figure 10 is a graphical representation of the state of stress and the Mohr-Coulomb failure criterion (c.f., Jaeger and Cook, 1976; Simpson, 1986) at a nominal depth of 1.8 km. In the presence of a fluid, the effective stress levels are reduced by the amount of the formation pore pressure which moves the Mohr circle to the left toward the failure envelope (middle circle, Figure 10). This condition is close to, but does not exceed the failure criterion for a fracture with no cohesion. Injection at a nominal pressure of 110 bars, however, would bring the zone immediately surrounding the well bottom to an effective stress state near critical for favorably oriented, preexisting fractures having cohesive strengths of as much as 40 bars and a friction coefficient near 0.6 (left circle, Figure 10). However, as the overburden pressure is only a lower bound for the estimate of the maximum compressive stress, the actual conditions for failure at the bottom of the wells may be more critical than the situation shown.

State of stress in the hypocentral region. The 31 January earthquake and nearly all its aftershocks were located about 12 km from the wells, and at depths of from

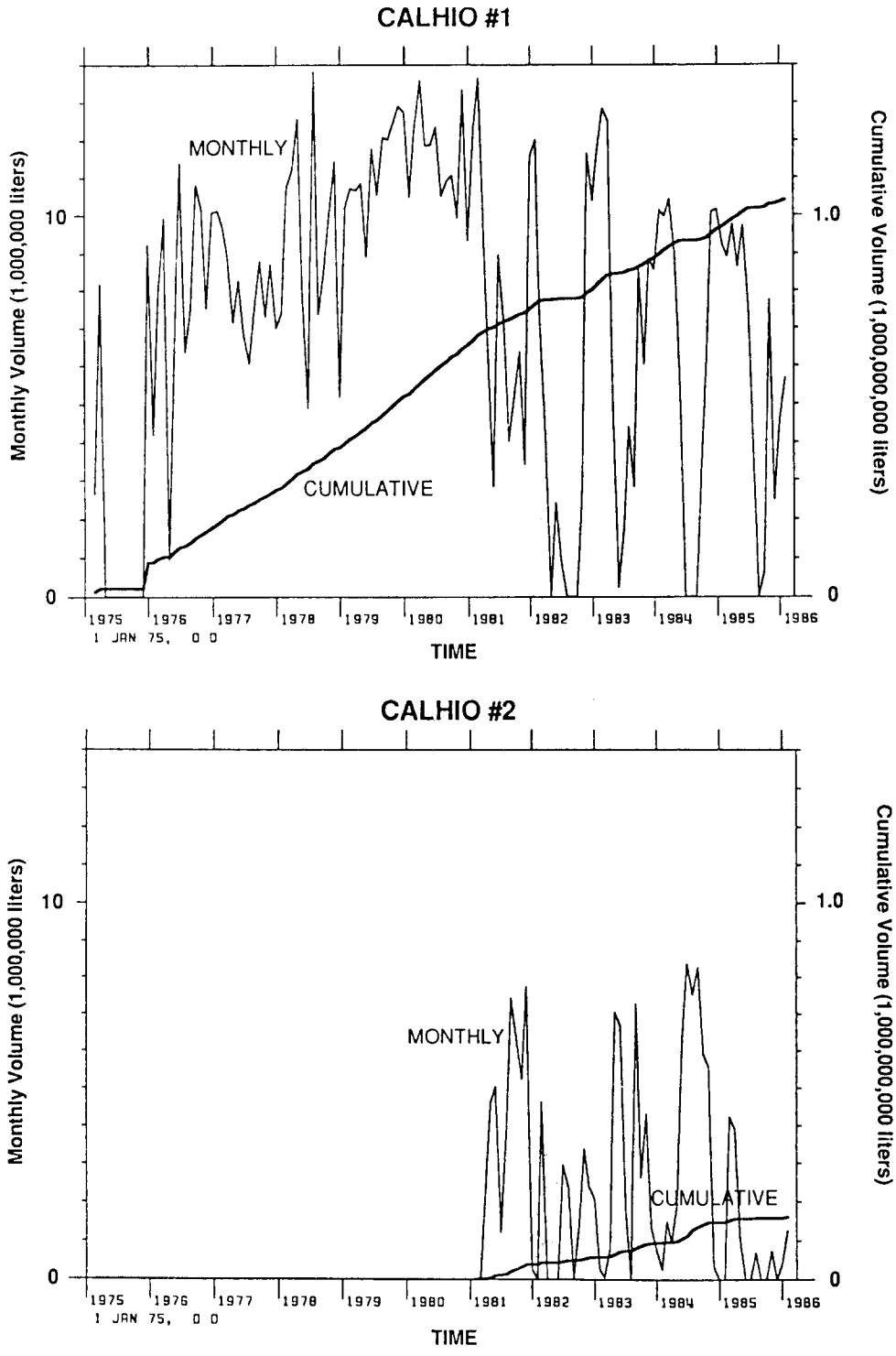

FIG. 9. Volume of fluid injected into the Calhio wells through time (Ohio EPA, written communication, 1986).

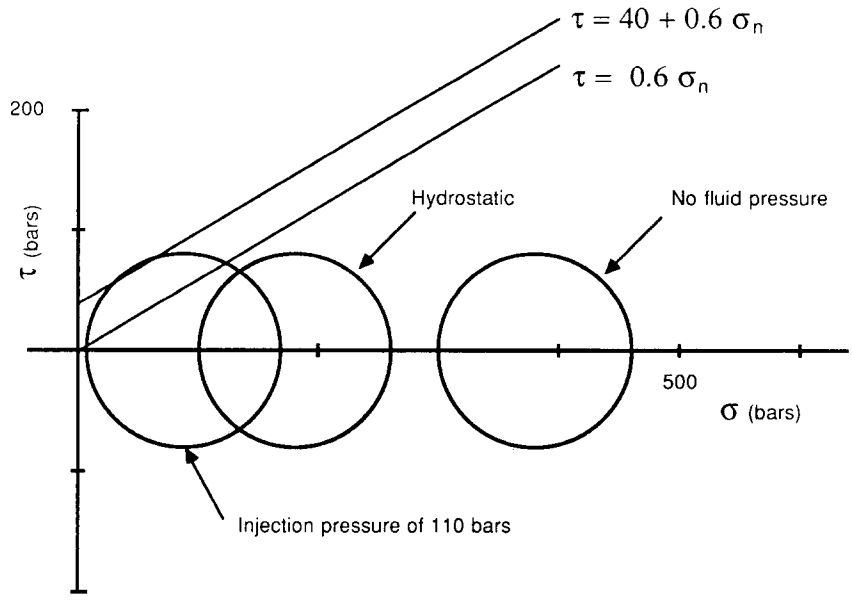

FIG. 10. Mohr circle diagram showing inferred state of stress at bottom of the injection wells (1.8 km depth).

2 to 6 km. Estimation of the existing state of stress at such increased hypocentral depths is difficult because simple extrapolation of principal stress components to depth is not theoretically justified, nor is there any indication that the stress ratio determined for the lower Paleozoic sedimentary section is maintained into the Precambrian granitic basement. What few measurements do exist for the basement (Michigan and Northern Illinois) indicate that the stress ratio of the minimum compressive stress over the vertical stress is between 0.72 to 0.77 (Haimson, 1978; Haimson and Doe, 1983). Such high stress ratios imply small stress differentials and consequently, stress conditions that are not as close to failure.

Fluid pressure changes resulting from injection

Estimates of the fluid pressure changes near the earthquake hypocenters are difficult to determine because little is known about the hydrologic properties of the basement where the earthquakes are actually occurring. The characteristics of the reservoir in the vicinity of the wells, however, can be estimated from measurements made during well completion. Using these characteristics, two types of reservoir models were evaluated in order to determine what the increase in fluid pressure near the earthquake hypocenters may have been as a result of the high-pressure fluid injection. The first type of model is an infinite isotropic reservoir; the second involves reservoirs of finite width (i.e., rectangular cross-section), but of infinite length, extending in the direction connecting the wells and the hypocenters. These models are for the purposes of studying how fluid pressure may have propagated horizontally away from the wells and do not address the question of how pressure effects could have migrated downward from the injection horizon to hypocentral depths (Figure 5, bottom).

Reservoir properties. For a given reservoir geometry, the fluid pressure field generated by injection is governed by the reservoir's transmissivity and storativity. In the case of the Calhio wells, waste fluid is injected into the essentially flat-lying

Maynardville and Mt. Simon formations at the base of the Paleozoic section. Porosities and permeabilities for the various formations, based on drill stem tests and core samples, are given in Table 5. Combining the two formations, a representative transmissitivity for the entire zone of injection is 4.2×10^{-6} m^2/sec. The storativity, which gives the amount of fluid released per unit column of aquifer for a unit decline in head, can be calculated from the expression

$$S = \rho g h(\alpha + n\beta) \tag{1}$$

where ρ is fluid density, h is the aquifer thickness, α is the vertical compressibility of the aquifer, n is the porosity, and β is the fluid compressibility. For a formation having the thickness of the Maynardville and Mt. Simon formations combined and a porosity of 0.08, setting $\alpha = 0$ in (1) yields a minimum storativity of 2.2×10^{-5}. The highest possible estimate of storativity corresponds to values of α greater than β, producing values for the storativity as high as 2.0×10^{-4}.

For purposes of calculating pressure 12 km from the well, it suffices to use an average fluid injection rate. The total volume injected into both wells is 1.17 billion liters (310 million gallons) during the period from March 1975 through November 1985 (Figure 9), corresponding to an average injection rate of 9.0 million liters/month. Because the distance between the wells (about 800 m) is small compared to the distance from the wells to the hypocenter, the two wells have been modeled as a single point source of fluid. For a given storativity (S), transmissivity (T) was adjusted so as to maintain the injection pressure at the well below the known maximum value of about 110 bars. In the models tested, injection was continued for a period of 12 yr (i.e., 1975 to 1986), after which flow was stopped in order to investigate the effects of ceasing injection.

Infinite reservoir model (radial flow). The pressure $p(r, t)$ at distance r, and time t as a result of a constant flow rate Q into a reservoir that extends uniformly in all directions is given by the equation

$$p(r, t) = \frac{\rho g Q}{4\pi T} \int_u^\infty \frac{e^{-\xi}}{\xi}\, d\xi \tag{2}$$

in which $u = r^2 S/4Tt$ (e.g., Freeze and Cherry, 1979). Evaluation of equation (2) for a hypothetical well of radius 12 cm, and upper and lower bounds to the storage coefficients, required transmissivities of 5.2×10^{-6} and 5.8×10^{-6} m^2/sec, respectively, in order to match the constraint of 110 bars injection pressure for the entire 12 yr of operation. The results for these two cases, in terms of pressure at the well head, are shown in Figure 11A as the two very similar curves labeled "infinite." Although the pressure at the well is not sensitive to the range of storage coefficient, the pressure at epicentral distances (Figure 11B) is affected. The minimum storativity yields a pressure increase of 3.6 bars 12 yr after injection initiation, but if the upper bound for the storage coefficient is assumed, the pressure increase at a distance of 12 km is only a fraction of a bar.

Note that in the hypothetical case that injection is stopped, pore pressure 12 km from the well (based on the radial flow model) continues to rise for at least 2 yr. This result confirms the insensitivty of pressure at this distance to the detailed time history of fluid injection at the well, and implies that if seismic activity is being induced by elevated pore pressure from the wells, it will not be suppressed immediately after ceasing injection.

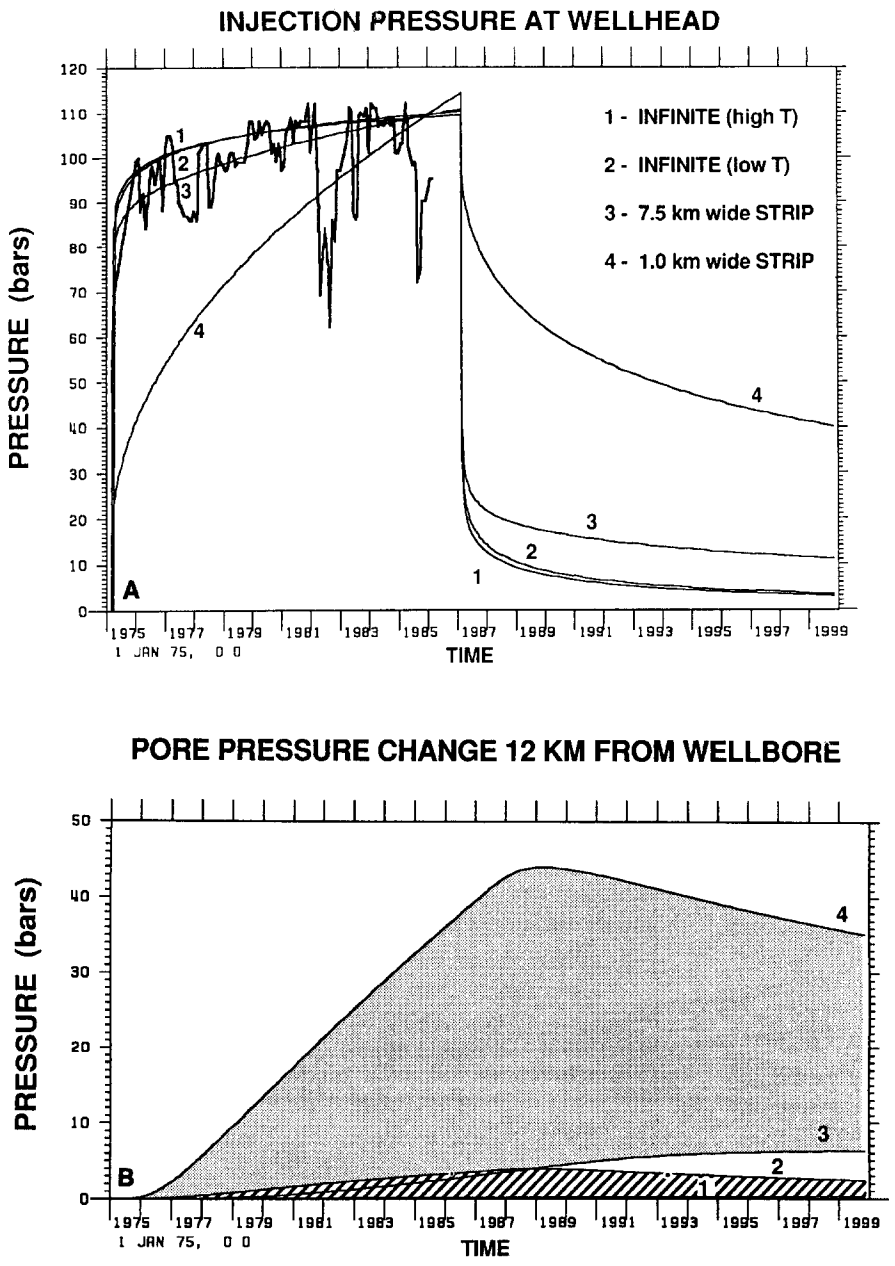

FIG. 11. Pressure versus time at wellhead (A) and 12 km from well bore (B) for both radial flow (infinite width) and finite-width reservoir models. An injection rate of 9 million liters/month is used and is assumed to cease after 12 yr. Curves labeled 1 and 2 represent transmissivities of 5.8×10^{-6} and $5.2 \times 10^{-6} m^2/sec$, respectively. Heavy solid line in (A) represents actual maximum pressures used at the Calhio wells (Ohio EPA, written communication, 1986). (B) The lower, *hachured area* is bounded above and below by curves obtained using the radial flow model, and maximum and minimum allowable storativities, respectively. The large, *shaded area* is bounded below by the pressure obtained using an infinite strip model 7.5 km wide (3), and above by that obtained using an infinite strip 1 km wide (4).

Infinite strip reservoir model. If fluid flow is confined to a narrow reservoir trending from the wells to the hypocentral region, then the pressure at a given distance from the well will be higher than for the radial flow models. This type of model was used by Hsieh and Bredehoeft (1981) to calculate the pressure distribution around the Rocky Mountain Arsenal well implicated in the 1960's Denver earthquake sequence. In the case of the Ohio earthquakes, there is no independent evidence that the injection zone has a long, narrow configuration. The calculations are still useful, however, in that they illustrate how large a pressure buildup at epicentral distances is possible and because they show how diagnostic the pressure history at the well bore is of the shape of the reservoir into which fluid is being injected.

For injection into the center of a strip of width w and infinite extent in the x direction, a constant injection rate Q produces a pressure given by

$$p(x, y, t) = \frac{\rho g Q}{4\pi T} \sum_{m=-\infty}^{\infty} \int_{u_m}^{\infty} \frac{e^{-\xi}}{\xi} d\xi \tag{3}$$

where $u_m = (x^2 + (y + mw)^2)S/4Tt$, and y is the distance from the center of the strip. Figure 11 shows pressure versus time at the well bore and at the epicentral distance of 12 km, respectively, for two infinite-strip reservoir models. Both strip reservoir models have storativities of 5.4×10^{-5} m^2/sec. One has a transmissivity equal to 6.0×10^{-6} m^2/sec and a width of 7.5 km; the other model has a higher transmissitivity of 2.5×10^{-5} m^2/sec and a width of 1 km. For the wider strip, pressure at the epicentral distance is comparable to that for the low storativity radial flow model, except that when injection stops, the pressure continues to rise to a higher value. For the narrow strip, pressure at the epicentral distance is about 36 bars 12 yr after beginning injection, and also continues to rise once injection ceases. Figure 11A demonstrates that analysis of the history of injection pressure can be used to discriminate the shape of the reservoir into which fluid is being injected. The actual increase in injection pressures with time, as measured in the Calhio #1 and #2 wells (Figure 11A, heavy line, Ohio EPA, written communication, 1986), more closely resembles the radial flow model and is inconsistent with the continually rapid increase in injection pressure required by the narrow-strip case.

Discussion

One of the more notable features of the aftershock sequence was that it contained so few events. No aftershocks were detected in the first 26 hr, and only 13 were reported by 15 April. This contrasts with other recent, moderate size earthquakes in the Eastern United States in which several tens to hundreds of aftershocks where detected in the weeks to months following the main shock (Herrmann *et al.*, 1982; Brown and Ebel, 1982; Wetmiller *et al.*, 1984; Seeber *et al.*, 1984). On the other hand, several earthquakes in the Central and Eastern United States have exhibited a remarkably similar lack of aftershock activity. Four aftershocks were found for the $m_b = 5.5$ earthquake in southern Illinois on 9 November 1968 (Stauder and Pitt, 1970), and the earthquake near Marked Tree, Arkansas, on 25 March 1976 (m_b = 5.0) had only two (m_b = 4.5 and m_{bLg} = 1.5) (Stauder *et al.*, 1976). The lack of aftershocks is thus neither discriminatory nor characteristic of noninduced earth quakes in the east, but is atypical of other earthquake sequences considered to have been triggered by fluid injection (e.g., Talwani and Acree, 1986).

The 31 January earthquake and all of its immediate aftershocks are rather tightly

clustered about 12 km south of the deep injection wells near Perry (Figure 5, top); however, there was one small microearthquake located close to the wells on 12 March. Its focal depth of 2 km corresponds to the base of the Paleozoic section and is the same depth at which fluid is injected from the Calhio wells (Figure 5, bottom). Small earthquakes in January and November of 1983 may also have occurred in close proximity to the Calhio wells and at shallow depths. Since the detection threshold for earthquakes near the wells prior to the installation of portable equipment following the 31 January earthquake (relying on the seismograph at John Carroll University) is estimated to be somewhat greater than magnitude 2.5, it is conceivable that additional small earthquakes could have occurred near the wells between the initiation of injection and the 31 January earthquake.

The time lag between the onset of the 1986 sequence and major injection well operations in Lake County (1975) is unusually long for typical cases of induced seismicity related to deep fluid injection, but is similar in some respects to several well-documented cases of earthquakes triggered by reservoir impoundment, particularly in those cases where the pressure front migrated a considerable distance prior to the onset of seismicity (Simpson, 1986). Further delays might be expected for diffusion of pore-pressure effects down to hypocentral depths. Permeabilities, as measured by pumping tests in the deep Ohio wells, are consistent with the observed time delay. Analysis of available stress measurements seems to indicate that the state of stress in northeastern Ohio is close to the theoretical threshold for small earthquakes as predicted by the Mohr-Coulomb failure criterion. This should not be surprising given the history of small to moderate earthquakes in the region. Since high-pressure fluid injection could have brought at least the region near the bottom of the wells into a critical stress state, the absence of large numbers of small earthquakes in the immediate vicinity of the wells suggests that there are not many favorably oriented, weak fractures near the wells. Thus, either existing fractures have cohesive strengths greater than 40 bars, or if weaker fractures do exist, they are not favorably oriented for failure in the existing stress field. The predominant dip of fractures observed in a core taken from the injection zone in Calhio well #2 is 20° (Resource Services Inc., 1980). Such fractures would not be as favorably oriented for failure, as shear stress is maximum only for near-vertical faults. Thus, the time between the initiation of injection (1975) and the 1986 earthquake could be related to the time required for pore-pressure effects to migrate out to an area with more favorably oriented fractures.

The actual pressure elevation in the hypocentral region as a result of the injection operation is certainly no more than 40 bars and more likely only a few bars. Although previously well-documented cases of seismicity induced by fluid injection typically involve pressure increases of several tens of bars, cases of reservoir-induced seismicity indicate that changes in water height of only a few meters, corresponding to pressure changes of less than a bar, have triggered substantial numbers of small earthquakes (Simpson, 1986). This result, combined with our lack of knowledge regarding the state of stress in the hypocentral region, makes it difficult to assess the minimum size of pore-pressure increase sufficient to haved triggered the 1986 earthquakes.

CONCLUSIONS

With our present information, it is not possible to confirm or reject the hypothesis that injection of waste into the Calhio wells triggered the 31 January earthquake and its aftershocks. If the state of stress in the hypocentral region is comparable to

that at the bottom of the injection wells, then it appears that elevating the pressure by a few tens of bars would have resulted in a state of effective stress that would be judged critical on the basis of the Mohr-Coulomb failure criterion. However, because these stress estimates are uncertain, and because they are not based on measurements made at the hypocenter, it is not possible to specify a level of pressure below which seismicity could not have been triggered, or above which earthquakes would necessarily be considered induced.

The state of stress in the lower sedimentary section is such that deep injection well operations could have elevated formation pore pressures sufficiently to trigger small shallow earthquakes, and two or possibly three small earthquakes did occur within the upper 2 km and in close proximity to the wells. However, the small pressure increase calculated for the hypocentral region of the main shock, its location in the Precambrian basement (where the stress regime may be different), the lack of large numbers of small earthquakes while formation pore pressure remains elevated, and the history of small to moderate earthquakes in the region prior to the initiation of injection all argue for a "natural" tectonic origin for the 31 January earthquake. Therefore, although triggering remains a possibility, the probability that fluid injection played a significant role in triggering the 31 January earthquake must be regarded as low.

Regardless of whether the 31 January earthquake is considered induced, the occurrence of the earthquake itself implies that the regional state of stress is near conditions for earthquake generation. In view of this situation, and of results in western New York (Fletcher and Sykes, 1977) and in southwestern Ontario (Mereu *et al.*, 1986), that suggest induced seismicity may be more prevalent in the northeast region that previously had been supposed, the possibility for future earthquake activity associated with injection operations in this region should be given continued attention. Plans are currently underway by John Carroll University and the Cleveland Electric Illuminating Company to continue monitoring seismicity in the Lake County area. Should additional activity occur near the wells, or between the wells and the 31 January earthquake, further examination of this issue would be warranted.

ACKNOWLEDGMENTS

This study was initially undertaken on behalf of, and with financial support from, the Office of Nuclear Reactor Regulation, U.S. Nuclear Regulatory Commission. This work was done while two of the authors (C. N. and E. R.) held National Research Council-U.S. Geological Survey Research Associateships. This paper benefited greatly from discussions with John Bredehoeft, Keith Evans, and Leon Reiter. The authors acknowledge and appreciate the cooperation, contributions, and exchange of data provided by a number of other groups involved in studies of the 31 January earthquake and its aftershocks, without which this paper could not have been prepared. Particularly helpful were: Roger Borcherdt, Gary Glassmoyer, Chuck Mueller, and Carlos Valdes for access to, and help with the GEOS data, and discovering the microearthquake of 12 March; Richard Holt, Gabriel LeBlanc, and Preston Turner for providing access to the considerable data set collected by Weston Geophysical; Tom Statton, Richard Quittmeyer, and Kathy Mroteck for generous access to the data collected by Woodward-Clyde Consultants; John Armbruster, Leonardo Seeber, and David Simpson for discussions and arrival-time data collected by the Lamont group; Robert Herrmann and Steve Neiers for providing their analysis of the main shock focal mechanism and data collected by St. Louis University; Jer-Ming Chiu for data collected by TEIC; Charles Langer, Margaret Hopper, Jim Dewey, and Russell Needham for arrival-time data, intensity results, location, and teleseismic first motions of the main shock; Horace Collins and Mike Hansen of the Ohio Geological Survey, and Dennis Crist and John Gray of Ohio DNR for information on local and regional subsurface geology, and data on the brine well in Painesville; Gerry Meyers of Ohio EPA for bringing to our attention the waste disposal wells in Lake County and providing considerable information on their operation; Warren Latimer and Jay Henthorn for providing well completion reports;

William Toth, Jim Rhodes, and Joe Fischer for additional information on the Calhio wells; Dale Wedge and Pat Linn of the Geauga County DSA for damage reports, and locations of the disturbed shallow water wells; and Pradeep Talwani for a preprint of this manuscript. We thank Jim Dewey, Dave Oppenheimer, Paul Segall, and an anonymous reviewer for their careful and thoughtful reviews of the manuscript.

REFERENCES

Borcherdt, R. D. (Editor) (1986). Preliminary report on aftershock sequence for the earthquake of January 31, 1986, near Painesville, Ohio, *U.S. Geol. Surv., Open-File Rept. 86-181*, 109 pp.

Borcherdt, R. D. and G. Glassmoyer (1987). On the aftershock sequence for the earthquake of January 31, 1986 in northeastern Ohio: effects of bandwidth and local geology on observed high-frequency ground motion, Paper Presented at Earthquake Groundmotion Estimation in Eastern North America, EPRI, March 31–April 2, Palo Alto, California, 46 pp.

Borcherdt, R. D., J. B. Fletcher, E. G. Jensen, G. L. Maxwell, J. R. VanSchaack, R. E. Warrick, E. Cranswick, M. J. S. Johnston, and R. McClearn (1985). A General Earthquake Observation System (GEOS), *Bull. Seism. Soc. Am.* **75**, 1783–1823.

Brown, E. J. and J. E. Ebel (1982). A study of selected aftershocks of the January, 1982 earthquake near Laconia, New Hampshire (abstract), *Earthquake Notes* **53**, 14.

Chaplin, M. P., S. R. Taylor, and M. N. Toksöz (1980). Coda-length magnitude scale for New England, *Earthquake Notes* **51**, 15–22.

Cleveland Electric Illuminating Company (1982). The Perry Nuclear Power Plant Units I and II: Final Safety Analysis Report, Cleveland, Ohio.

Clifford, M. J. (1973). Silurian rock salt of Ohio, *Ohio Geol. Surv. Rept. of Investigations*, vol. 9, Columbus, Ohio, 42 pp.

Dewey, J. W. and D. W. Gordon (1984). Map showing recomputed hypocenters of earthquakes in the eastern and central United States and adjacent Canada, 1925–1980, U.S. Geol. Surv. Map MF-1699.

Dunrud, C. R. and B. B. Nevins (1981). Solution mining and subsidence in evaporite rocks in the United States, U.S. Geol. Surv. Map I-1298.

Dziewonski, A. M. (1986). Global seismicity of 1985 (abstract), *EOS, Trans. Am. Geophys. Union* **67**, 309.

Evans, K. (1987). *In-situ* stress discontinuity across the Appalachian Plateau decollement (abstract), Paper Presented at AGU Spring Meeting, Baltimore, Maryland, p. 66.

Fletcher, J. B. and L. R. Sykes (1977). Earthquakes related to hydraulic mining and natural seismic activity in western New York State, *J. Geophys. Res.* **82**, 3767–3780.

Freeze, R. A. and J. A. Cherry (1979). *Ground Water*, Prentice-Hall Inc., Englewood Cliffs, New Jersey, 604 pp.

Glassmoyer, G., R. Borcherdt, J. King, C. Dietal, E. Sembera, E. Roeloffs, C. Valdes, and C. Nicholson (1986). Source and propagation characteristics of aftershock sequence near Painesville, Ohio (abstract), *EOS, Trans. Am. Geophys. Union* **67**, 314.

Haimson, B. C. (1978). Crustal stress in the Michigan basin, *J. Geophys. Res.* **83**, 5857–5863.

Haimson, B. C. and T. W. Doe (1983). State of stress, permeability, and fractures in the Precambrian granite of northern Illinois, *J. Geophys. Res.* **88**, 7355–7372.

Healy, J. H., W. W. Rubey, D. T. Griggs, and C. B. Raleigh (1968). The Denver earthquakes, *Science* **161**, 1301–1309.

Herrmann, R. B. and B. V. Nguyen (1986). Focal mechanism studies of the January 31, 1986 Perry Ohio earthquake (abstract), *Earthquake Notes* **57**, 107.

Herrmann, R. B., C. A. Langston, and J. E. Zollweg (1982). The Sharpsburg, Kentucky, earthquake of 27 July, 1980, *Bull. Seism. Soc. Am.* **72**, 1219–1239.

Hickman, S. H., J. H. Healy, and M. D. Zoback (1985). *In situ* stress, natural fracture distribution, and borehole elongation in the Auburn geothermal wall, Auburn, New York, *J. Geophys. Res.* **90**, 5497–5512.

Hildenbrand, T. G. and R. P. Kucks (1984a). Residual total intensity magnetic map of Ohio, U.S. Geol. Surv. Map GP-961.

Hildenbrand, T. G. and R. P. Kucks (1984b). Complete Bouguer gravity anomaly map of Ohio, U.S. Geol. Surv. Map GP-962.

Hsieh, P. A. and J. D. Bredehoeft (1981). A reservoir analysis of the Denver earthquakes: a case of induced seismicity, *J. Geophys. Res.* **86**, 903–920.

Jaeger, J. C. and N. C. W. Cook (1976). *Fundamentals of Rock Mechanics*, John Wiley and Sons, Inc., New York, 585 pp.

Lahr, J. C. (1985). HYPOELLIPSE/VAX: a computer program for determining local earthquake hypocentral parameters, magnitude and first-motion pattern, *U.S. Geol. Surv., Open-File Rept. 84-519*, 35 pp.

Mereu, R. F., J. Brunet, K. Morrissey, B. Price, and A. Yapp (1986). A study of the microearthquakes of the Gobles oil field area of southwestern Ontario, *Bull. Seism. Soc. Am.* **76,** 1215–1223.

Musman, S. A. and T. Schmidt (1986). The relationship of intraplate seismicity to continental scale strains (abstract), *EOS, Trans. Am. Geophys. Union* **67,** 307.

Natural Resources Management Corp. (1971). Report on the drilling, testing and completion of the subsurface disposal well #1, Calhio Chemicals, Inc., Perry, Ohio, 81 pp.

NEIC (1986). Preliminary determination of epicenters—Monthly listing: January, 1986, *U.S. Geol. Surv. Bulletin*, 24 pp.

Nuttli, O. W., W. Stauder, and C. Kisslinger (1969). Travel time tables for earthquakes in the central United States, *Earthquake Notes* **40,** 19–28.

Petro Evaluation Services, Inc. (1985). Well completion record, saltwalter injection well, Painesville, Lake County, Ohio, 5 pp.

Press, F. (1966). Seismic velocities, in *Handbook of Physical Constants*, S. D. Clark, Editor, *Geol. Soc. Am. Mem.* **97,** 195–218.

Raleigh, C. B., J. H. Healy, and J. D. Bredehoeft (1976). An experiment in earthquake control at Rangely, Colorado, *Science* **191,** 1230–1237.

Reasenberg, P. and D. Oppenheimer (1985). FPFIT, FPPLOT and FPPAGE: Fortran computer programs for calculating and displaying earthquake fault-plane solutions, *U.S. Geol. Surv., Open-File Rept. 85-739*, 109 pp.

Resources Services, Inc. (1980). Report on the drilling, testing and completion of the subsurface disposal well, Injection Well #2, Calhio Chemicals, Inc., Perry, Ohio, 84 pp.

Rice, J. R. and M. P. Cleary (1976). Some basic stress diffusion solutions for fluid-saturated elastic porous media with compressible constituents, *Rev. Geophys. Space Phys.* **14,** 227–241.

Roeloffs, E. (1987). Hydrologic precursors: a review, Paper Presented at Physical and Observational Basis for Intermediate-Term Earthquake Prediction, U.S. Geological Survey Redbook Conference, Monterey, California, 34 pp.

Roeloffs, E. and J. D. Bredehoeft (1985). Coseismic response of water wells near Parkfield, California, to the August 4, 1985 North Kettleman Hills earthquake (abstract), *EOS, Trans. Am. Geophys. Union* **66,** 986.

Root, S. I. and R. H. MacWilliams (1986). The Suffield fault, Stark County, Ohio, *Ohio J. Sci.* **86,** 161–163.

Sbar, M. L. and L. R. Sykes (1973). Contemporary compressive stress and seismicity in eastern North America: an example of intra-plate tectonics, *Geol. Soc. Am. Bull.* **84,** 1861–1882.

Seeber, L., E. Cranswick, J. Armbruster, and N. Brastow (1984). The October 1983 Goodnow, N.Y., aftershock sequence: regional seismicity and structural features in the Adirondacks (asbtract), *EOS, Trans. Am. Geophys. Union* **65,** 239.

Simpson, D. W. (1986). Triggered earthquakes, *Ann. Rev. Earth Planet Sci.* **14,** 21–42.

Stauder, W. and A. M. Pitt (1970). Note on an aftershock study, south central Illinois earthquake of November 9, 1968, *Bull. Seism. Soc. Am.* **60,** 983–986.

Stauder, W., S. Schaefer, J. Best, and S. T. Morrissey (1976). *Southeast Missouri Regional Seismic Bulletin*, vol. 7, St. Louis University, St. Louis, Missouri, 25 pp.

Stauder, W., R. Herrmann, S. Singh, C. Nicholson, D. Reidy, R. Perry, S. Morrissey, and E. Haug (1981). Central Mississippi Valley earthquakes—1979, *Earthquake Notes* **52,** 26–31.

Stover, C. W., B. G. Reagor, and S. T. Algermissen (1979). Seismicity map of the state of Ohio, U.S. Geol. Surv. Map MF-1142.

Talwani, P. and S. Acree (1986). Deep well injection at the Calhio wells and the Leroy, Ohio earthquake of January 31, 1986, A report to the Cleveland Electric Illuminating Co., Cleveland, Ohio, 92 pp.

Vorhis, R. C. (1968). Effects outside Alaska, in *The Great Alaska Earthquake of 1964: Hydrology*, Part A, National Academy of Sciences Publication 1603, 140–189.

Wakita, H. (1975). Water wells as possible indicators of tectonic strain, *Science* **189,** 553–555.

Wesson, R. L. and C. Nicholson (1986). Studies of the January 31, 1986 northeastern Ohio earthquake: a report to the U.S. Nuclear Regulatory Commission, *U.S. Geol. Surv., Open-File Rept. 86-331*, 131 pp.

Weston Geophysical Corporation (1986). Investigations of confirmatory seismological and geological issues: northeastern Ohio earthquake of January 31, 1986, A report to the Cleveland Electric Illuminating Co., Cleveland, Ohio, 233 pp.

Weston Geophysical Corporation (1987a). Quarterly progress report, CEI seismic monitoring program

for northeastern Ohio, Octoger 15, 1986–January 15, 1987, A report prepared for Cleveland Electric Illuminating Company, Cleveland, Ohio, 12 pp.

Weston Geophysical Corporation (1987b). Second quarterly report, CEI seismic monitoring network, January 15–April 15, 1987, A report prepared for Cleveland Electric Illuminating Company, Cleveland, Ohio, 11 pp.

Wetmiller, R. J., J. Adams, F. M. Anglin, H. S. Hasegawa, and A. E. Stevens (1984). Aftershock sequences of the 1982 Miramichi, New Brunswick earthquakes, *Bull. Seism. Soc. Am.* **74**, 621–653.

Zoback, M. L. and M. Zoback (1980). Interpretative stress map of the conterminous United States, *J. Geophys. Res.* **85**, 6113–6156.

U.S. GEOLOGICAL SURVEY
RESTON, VIRGINIA (C.N., R.L.W.)

U.S. GEOLOGICAL SURVEY
MENLO PARK, CALIFORNIA (E.R.)

Manuscript received 2 February 1987

ADDENDUM

Subsequent monitoring in the Lake County region by Weston Geophysical on behalf of Cleveland Electric Illuminating Company has detected 13 more microearthquakes during the period 15 April 1986 to 15 April 1987 (Weston Geophysical, 1987a, b). Three of these events are located within the previously defined aftershock cluster of the 31 January 1986 earthquake (Figure A1, top). One earthquake occurred less than 3 km east of the brine injection well (SALT, Figure A1) north of Painesville. The other nine microearthquakes occurred within 5 km of the deep injection wells operated by Calhio and all at depths of 2 km or less (Figure A1, top and bottom). Magnitudes of these small events are all about $M_c = 1.0$ or less. The distance of these later earthquakes from the Calhio wells (<5 km) corresponds to an inferred pore-pressure increase of at least 15 bars (Figure A1, middle). An increase of 15 bars fluid pressure corresponds with the pore-pressure increase calculated to trigger slip on favorably oriented, weak fractures, based on our inferred values of the principal stress components (see Figure 10) These results suggest that the state of stress in northeastern Ohio is sufficiently close to failure that elevating formation pore pressure by a few tens of bars can trigger small shallow earthquakes. A recent compilation of relative stress values (Evans, 1987) indicates that similar stress conditions near the base of the Paleozoic section prevail over much of the Appalachian plateau.

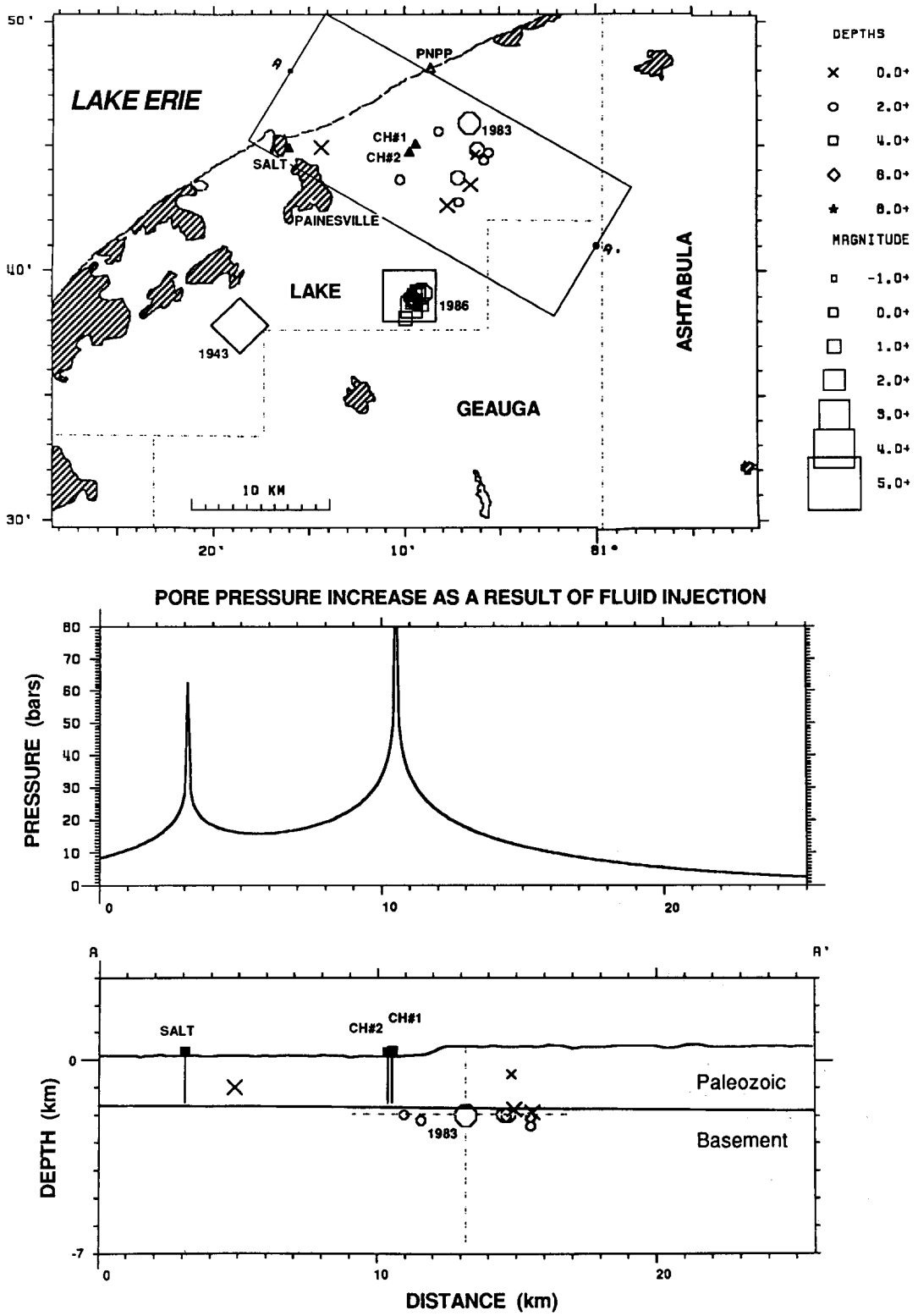

FIG. A1. (*Top*) Map of northeastern Ohio showing the Perry Nuclear Power Plant (PNPP), the deep fluid injection wells (solid triangles) in Lake County, and recent seismicity through 15 April 1987. (*Middle*) Maximum increase in pore pressure resulting from fluid injection, as projected along the hypothetical profile *A–A'*, assuming radial flow, minimum reservoir storativities, and injection rates of 2 and 9 million liters/month at the brine (SALT) and Calhio (CH#1 and CH#2) wells for the last 2 and 12 yr, respectively. (*Bottom*) Vertical cross-section along *A–A'*, no exaggeration, for the seismicity located within the rectangle shown on the map.